

# DAPK1 Interaction with NMDA Receptor NR2B Subunits Mediates Brain Damage in Stroke

Weihong Tu,<sup>1,2,4</sup> Xin Xu,<sup>1,4</sup> Lisheng Peng,<sup>1</sup> Xiaofen Zhong,<sup>1</sup> Wenfeng Zhang,<sup>3</sup> Mangala M. Soundarapandian,<sup>2</sup> Cherine Balel,<sup>2</sup> Manqi Wang,<sup>1</sup> Nali Jia,<sup>1</sup> Wen Zhang,<sup>1</sup> Frank Lew,<sup>2</sup> Sic Lung Chan,<sup>2</sup> Yanfang Chen,<sup>3</sup> and Youming Lu<sup>1,2,\*</sup>

<sup>1</sup>Department of Neurology and Neuroscience Center, Louisiana State University Health Sciences Center School of Medicine, New Orleans, LA 70112, USA

<sup>2</sup>Biomedical Sciences Center, Burnett School of Biomedical Sciences, College of Medicine, University of Central Florida, Orlando, FL 32816, USA

<sup>3</sup>Department of Pharmacology and Toxicology, Wright State University Boonshoft School of Medicine, Dayton, OH 45435, USA

<sup>4</sup>These authors contributed equally to this work

\*Correspondence: ylu1@lsuhsc.edu

DOI 10.1016/j.cell.2009.12.055

## SUMMARY

*N*-methyl-*D*-aspartate (NMDA) receptors constitute a major subtype of glutamate receptors at extrasynaptic sites that link multiple intracellular catabolic processes responsible for irreversible neuronal death. Here, we report that cerebral ischemia recruits death-associated protein kinase 1 (DAPK1) into the NMDA receptor NR2B protein complex in the cortex of adult mice. DAPK1 directly binds with the NMDA receptor NR2B C-terminal tail consisting of amino acid 1292-1304 (NR2B<sub>CT</sub>). A constitutively active DAPK1 phosphorylates NR2B subunit at Ser-1303 and in turn enhances the NR1/NR2B receptor channel conductance. Genetic deletion of DAPK1 or administration of NR2B<sub>CT</sub> that uncouples an activated DAPK1 from an NMDA receptor NR2B subunit in vivo in mice blocks injurious Ca<sup>2+</sup> influx through NMDA receptor channels at extrasynaptic sites and protects neurons against cerebral ischemic insults. Thus, DAPK1 physically and functionally interacts with the NMDA receptor NR2B subunit at extrasynaptic sites and this interaction acts as a central mediator for stroke damage.

## INTRODUCTION

Glutamate is the major excitatory transmitter in the mammalian central nervous system (CNS) and plays an essential role in neural development, excitatory synaptic transmission, and plasticity (Greengard, 2001). Immediately following ischemia, however, glutamate accumulates at synapses (Drejer et al., 1985; Rossi et al., 2000), resulting in extensive stimulation of its receptors that can eventually be toxic to neurons (Lipton, 2006; Lo et al., 2003). Glutamate activates three classes of iono-

phore-linked postsynaptic receptors, namely N-methyl-*D*-aspartate (NMDA) and  $\alpha$ -amino-3-hydroxy-5-methyl-4-isoxazole propionic acid (AMPA) and kainate receptors. NMDA receptor toxicity is dependent on extracellular Ca<sup>2+</sup>, and reflects a large amount of Ca<sup>2+</sup> influx directly through the receptor-gated ion channels (Simon et al., 1984; for review, see Lipton, 2006; Lo et al., 2003). As most AMPA receptor channels have poor Ca<sup>2+</sup> permeability, injury may result primarily from indirect Ca<sup>2+</sup> entry through voltage-gated Ca<sup>2+</sup> channels, Ca<sup>2+</sup>-permeable acid-sensing ion channels (Xiong et al., 2004), and possibly via a cleavage of Na<sup>+</sup>/Ca<sup>2+</sup> exchangers (Bano et al., 2005). Ca<sup>2+</sup> overload triggers several downstream lethal reactions including nitrosative stress (Aarts et al., 2003; Uehara et al., 2006), oxidative stress (Kinouchi et al., 1991) and mitochondrial dysfunction (Krajewski et al., 1999; Fiskum et al., 1999). Thus, over-stimulation of glutamate receptors can be considered as a primary intracellular event that induces neuronal death in stroke.

NMDA receptors constitute the major subtype of glutamate receptors, and normally participate in rapid excitatory synaptic transmission. To date, a variety of NMDA receptor subunit proteins (NR1, NR2A–D) have been cloned (Madden, 2002). Native NMDA receptors appear to be heterooligomeric complexes consisting of an essential NR1 subunit and one or more regulatory NR2 subunits (NR2A–D) and possibly the more recently identified NR3 subunit (Chatterton et al., 2002). Since the NR2C- (and possibly NR2D-) containing receptors have very low probability for their channel opening (Sprengel et al., 1998), both NR2A- and NR2B-containing NMDA receptors are considered as the main types of functional NMDA receptor channels in CNS neurons (Madden, 2002). Activation of NMDA receptors requires two coincident events: 1) binding to the coagonists of glutamate and glycine, and 2) simultaneous membrane depolarization, which removes the Mg<sup>2+</sup> block of the channel pore, leading to the influx of Ca<sup>2+</sup>. Under physiological conditions, the entrance of Ca<sup>2+</sup> produces partial inhibition of NMDA receptors via Ca<sup>2+</sup>-dependent inactivation, thereby preventing the intracellular Ca<sup>2+</sup> overload (Krupp et al., 1999). Under

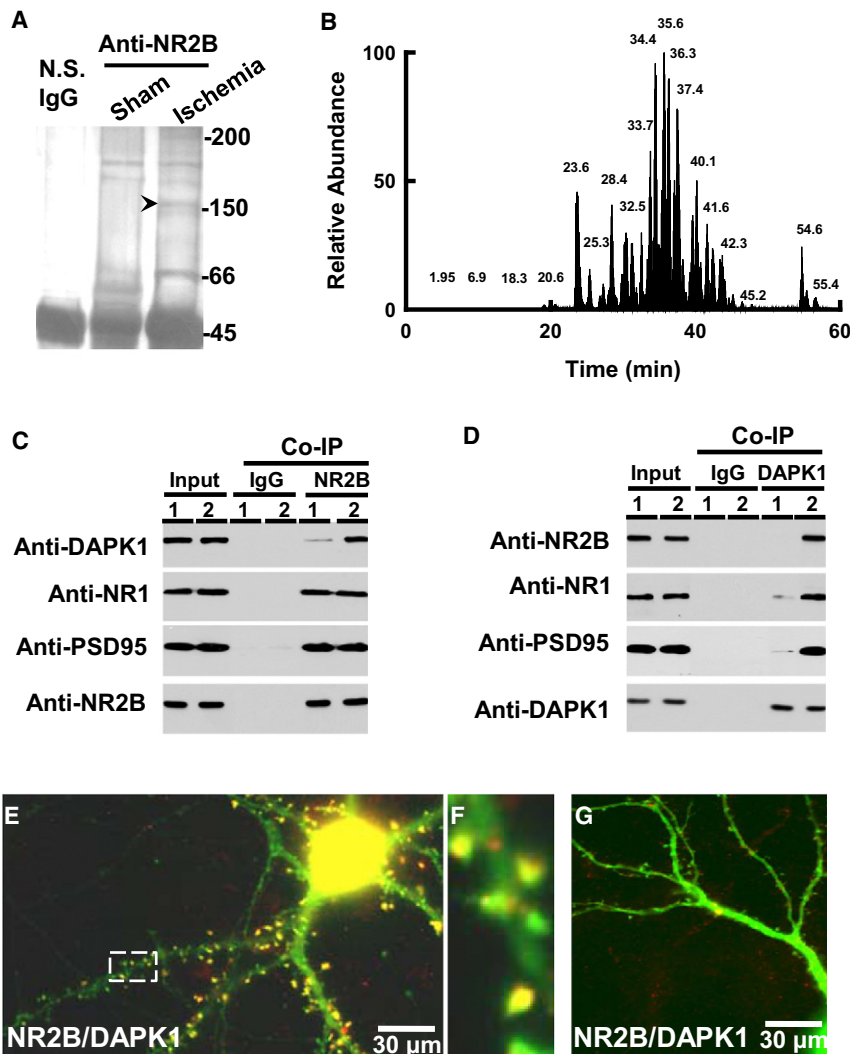


**Figure 1. Ischemia Recruits DAPK1 into NMDA Receptor Complex**

(A) The immune-precipitates with nonspecific IgG (N.S. IgG), or antibody against NMDA receptor NR2B subunit (anti-NR2B) in the membrane extracts (5 mg proteins) from the cortex of mice 2 hr after operation for sham or MCAO (Ischemia) were stained with Coomassie blue.

(B) Base peak chromatogram from trypsin-digested products of a selected protein band (arrow head in [A]).

(C and D) The membrane extracts (1 mg proteins) from the cortex of mice 2 hr after sham (lane 1) or MCAO (lane 2) were precipitated with nonspecific IgG (IgG) or anti-NR2B (C) or anti-DAPK1 (D) and probed with anti-DAPK1, anti-NR1, anti-PSD95 or anti-NR2B. Input: 20  $\mu$ g of protein was loaded in each lane except the PSD95 lane, in which 10  $\mu$ g proteins were loaded.

(E–G) DAPK1<sup>+/+</sup> (E) and DAPK1<sup>-/-</sup> (G) cultured neurons were stained with anti-DAPK1 (red) and anti-NR2B (green). A high magnified image (F) from a selected area in (E). In panels A–G, similar results were observed in each of the four experiments.

See also Figure S1.

## RESULTS

### Cerebral Ischemia Recruits DAPK1 into NMDA Receptor NR2B Protein Complex

To explore the cell death signals that are linked with NMDA receptors in stroke damage, we used anti-NMDA receptor NR2B antibodies to precipitate the NMDA receptor complex in the membrane extracts from the cortex of mice that had been subjected to focal cerebral ischemia or sham operation (for details,

see [Experimental Procedures](#)). The precipitates from both groups were separated on the SDS-PAGE and stained with Coomassie blue ([Figures 1A and 1B](#)). Compared to the control group, the additional protein bands on the gel with estimated size of 66 kDa and 150 kDa were observed in the ischemic group. We then analyzed the protein components in these bands using a reverse phase Nano-Liquid Chromatography-Tandem Mass Spectrometry (NLC/MS) approach. Five peptide sequences: AEQHEHVAGLLAR, DKSGETALAVAAR, GLFFQQLRPTQNLQPR, HYLSPQQLR, and RGVSRDIER, were found to match death-associated protein kinase 1 (DAPK1, see [Tables S1 and S2](#)). We next probed the precipitates with antibody against DAPK1 and confirmed the existence of endogenous DAPK1 in the NMDA receptor complex ([Figure 1C](#), see also [Figure S1](#)). We also carried out the reciprocal coimmunoprecipitation, in which anti-DAPK1 was used to precipitate NMDA receptor NR1, NR2B subunits, and their functional interacting partner PSD-95, and CaMK-II ([Figure 1D](#)). Single neuronal labeling demonstrated a colocalization of DAPK1 with NMDA receptor NR2B subunits

pathological conditions, however, this negative feedback in Ca<sup>2+</sup> regulation of NMDA receptors is disabled, resulting in excessive Ca<sup>2+</sup> influx through the receptor channels ([Wang et al., 2003a](#)). Ca<sup>2+</sup> overload triggers multiple intracellular catabolic processes, and thus induces an irreversible death of neuronal cells in the brain (for review, see [Lipton, 2006](#); [Lo et al., 2003](#)).

Although over stimulation of NMDA receptors contributes to ischemic neuronal death, blocking them totally could be deleterious to animals and humans because targeting these receptors also blocks the physiological actions of the receptor as well. In the present study, we report that DAPK1, or death-associated protein kinase 1, acts as a specific “cell death signal” that couples NMDA receptor channels at extrasynaptic sites to ischemic neuronal death. We also demonstrate that uncoupling of an activated DAPK1 from the NMDA receptor complex protects against brain damage in stroke without affecting the physiological actions of the NMDA receptors. Thus, targeting DAPK1-NMDA receptor interaction can be considered as a practical strategy for stroke therapy.

see [Experimental Procedures](#)). The precipitates from both groups were separated on the SDS-PAGE and stained with Coomassie blue ([Figures 1A and 1B](#)). Compared to the control group, the additional protein bands on the gel with estimated size of 66 kDa and 150 kDa were observed in the ischemic group. We then analyzed the protein components in these bands using a reverse phase Nano-Liquid Chromatography-Tandem Mass Spectrometry (NLC/MS) approach. Five peptide sequences: AEQHEHVAGLLAR, DKSGETALAVAAR, GLFFQQLRPTQNLQPR, HYLSPQQLR, and RGVSRDIER, were found to match death-associated protein kinase 1 (DAPK1, see [Tables S1 and S2](#)). We next probed the precipitates with antibody against DAPK1 and confirmed the existence of endogenous DAPK1 in the NMDA receptor complex ([Figure 1C](#), see also [Figure S1](#)). We also carried out the reciprocal coimmunoprecipitation, in which anti-DAPK1 was used to precipitate NMDA receptor NR1, NR2B subunits, and their functional interacting partner PSD-95, and CaMK-II ([Figure 1D](#)). Single neuronal labeling demonstrated a colocalization of DAPK1 with NMDA receptor NR2B subunits

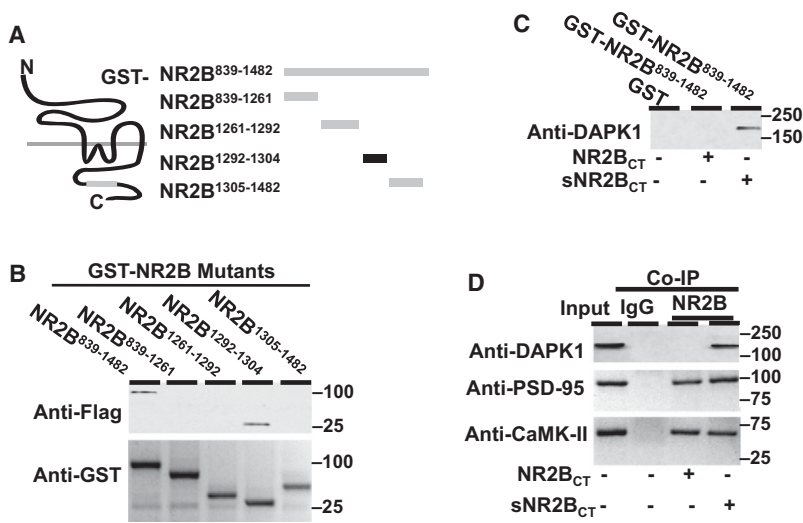


**Figure 2. DAPK1 Directly Binds to NMDA Receptor NR2B Subunit**

(A) Representation illustrates a series of GST fusion proteins with the NR2B C-terminal mutants. (B) Affinity binding assay shows that flag-tagged catalytic domain of DAPK1 binds with GST-NR2B<sup>839-1482</sup> (~100 kDa) and GST-NR2B<sup>1292-1304</sup> (~30 kDa). The blots show anti-Flag (top) and anti-GST (bottom).

(C) NR2B<sub>CT</sub> suppresses DAPK1 association with NMDA receptor NR2B subunit. Membrane extracts (500 μg proteins) from the forebrain of mice 2 hr after MCAO were incubated with GST or the GST-NR2B<sub>CT</sub><sup>839-1482</sup> in the presence of 50 μM NR2B<sub>CT</sub> or sNR2B<sub>CT</sub> and probed with anti-DAPK1.

(D) NR2B<sub>CT</sub> blocks NMDA receptor association with DAPK1 but not with PSD-95. Membrane extracts were precipitated with nonspecific IgG (IgG) or anti-NR2B in the presence of 50 μM NR2B<sub>CT</sub> or sNR2B<sub>CT</sub> and probed with anti-DAPK1, or anti-PSD-95, or anti-CaMK-IIα. Input: 50 μg of protein was loaded in each lane. In (B)–(D), similar results were observed in each of the four experiments.

at the post-synaptic spines (Figures 1E–1G). Thus, DAPK1 is physically associated with NMDA receptors.

To identify a direct binding region of NMDA receptor NR2B subunit with DAPK1, we generated a series of NMDA receptor NR2B C-terminal deletion mutants fused with glutathione-S-transferase (GST, Figure 2A). We found that only the NR2B<sup>1292-1304</sup> fragment was capable of binding with DAPK1 (Figure 2B). The NR2B<sup>1292-1304</sup> fragment contains a consensus binding motif (R/K[R/K][R/KXXRXXSX]) of DAPK1 with only one mismatch residue at asparagine-1296 (Schumacher and Schavocky, 2004). We subsequently synthesized a NR2B C-terminal tail peptide of <sup>1292</sup>KKNRNKLRHQHSY<sup>1304</sup> (NR2B<sub>CT</sub>). Application of 50 μM NR2B<sub>CT</sub> uncoupled an activated DAPK1 from NMDA receptor NR2B protein complex (Figure 2C), but it did not affect the association of PSD-95 or CaMK-II with the NMDA receptor NR2B subunit (Figure 2D).

### DAPK1 Activation Enhances the NR1/NR2B Channel Conductance

Having determined a binding domain of DAPK1 with the NMDA receptor NR2B subunit, we then examined whether DAPK1 functionally regulates NMDA receptor channel activity. We coexpressed the NR1/NR2B receptors with a constitutively active DAPK1 (cDAPK1), or the wild-type DAPK1 (wDAPK1) in HEK293 cells. We found that cDAPK1 increased the peak amplitude of the recombinant NR1/NR2B receptor currents (Figure 3A), but not the NR1/NR2A receptor currents (Figure 3B), at a range of holding potentials from –100 to +100 mV. Since the decay time constants and the reversal potentials were not changed (Figure 3A), cDAPK1 specifically increases the recombinant NR1/NR2B receptor channel conductance. To determine whether enhancement of NR1/NR2B receptor currents is mediated directly by DAPK1-NR2B interaction, we made use of NR2B subunit C-terminal peptide, NR2B<sub>CT</sub>, at a concentration of 10, 25, or 50 μM, which was diffused directly into the recording cells via patch electrode (Figure 3C). After a 10 min diffusion of 50 μM NR2B<sub>CT</sub>, the peak amplitude of the whole-cell currents decreased by  $0.56 \pm 0.086$  of the baseline (mean  $\pm$  standard error of the mean [SEM], Figure 3C). A peptide

with the same amino acid composition but in random order scrambled NR2B<sub>CT</sub> (sNR2B<sub>CT</sub>) served as control, and did not reduce the recombinant NR1/NR2B receptor currents ( $0.98 \pm 0.11$  of the baseline, mean  $\pm$  SEM). Whole-cell currents in HEK293 cells coexpressing NR1/NR2B with wDAPK1 were not affected by 50 μM NR2B<sub>CT</sub> (Figure 3D). Thus, enhancement of the recombinant NR1/NR2B receptor channel conductance is mediated by activated DAPK1 binding with NR2B subunit.

### DAPK1 Activation Phosphorylates NR2B Subunit at Ser-1303

We next examined whether an activated DAPK1 phosphorylates NR2B subunit at Ser-1303, (Figure 3E), a residue corresponding to a phosphorylation site (KXXRXXSX) of DAPK1 (Schumacher and Schavocky, 2004). We coexpressed wDAPK1 or cDAPK1 in HEK293 cells with the recombinant NR1/NR2B or the mutant NR1/NR2BS<sup>1303A</sup> receptors. In the mutant NR2BS<sup>1303A</sup>, a Ser-1303 residue was replaced with an alanine (A). The levels of phosphorylation at Ser-1303 ( $pS^{1303}$ ) were measured using antibody against the  $pS^{1303}$  (anti- $pS^{1303}$ ). The anti- $pS^{1303}$  recognized the recombinant wide NR2B subunit, but not with the mutant NR2BS<sup>1303A</sup>, demonstrating the specificity of anti- $pS^{1303}$  reaction (Figure 3E). To determine whether phosphorylation of NR2B at Ser-1303 is sufficient to modulate the NR1/NR2B receptor channel activity, whole-cell currents were recorded from HEK293 cells coexpressing the NR1/NR2B or the mutant NR1/NR2BS<sup>1303A</sup> with wDAPK1 (Figure 3F) or cDAPK1 (Figure 3G). We found that cDAPK1 increased the peak amplitude of the recombinant NR1/NR2B receptor currents, but not the mutant NR1/NR2BS<sup>1303A</sup> receptor currents, at a range of holding potentials from –80 to +80 mV (Figure 3G). Thus, an activated DAPK1 enhances NR1/NR2B receptor channel conductance by phosphorylating NR2B subunit at Ser-1303.

### Generation of Null Mutant Mice Lacking the DAPK1 Gene

To determine whether an activated DAPK1 physically and functionally interacts with synaptic NMDA receptor NR2B subunit in vivo, we generated null mutant mice with deficiency in

expression of DAPK1 (DAPK1<sup>-/-</sup> mice).  $\beta$ -gal, a marker for DAPK1 deletion, was observed throughout the brain of the DAPK1<sup>-/-</sup> mice, including the cortex and hippocampus (Figure 4A). RT-PCR and western blot analysis revealed undetectable levels of DAPK1 mRNA (Figure 4B) and proteins (Figure 4C) in the DAPK1<sup>-/-</sup> mice. No difference of DAPK2 and DAPK3 proteins was observed between DAPK1<sup>-/-</sup> and DAPK1<sup>+/+</sup> mice (Figure 4D).

We next surveyed several synaptic proteins, including AMPA receptor subunits GluR1 and GluR2, and NMDA receptor subunits NR1, NR2A, and NR2B and PSD-95 (Figure 4D). We confirmed that genetic deletion of DAPK1 does not alter the overall synaptic protein compositions in the brain. We next examined synaptic transmission in the CA1 hippocampus. We analyzed excitatory post-synaptic currents (EPSCs). By plotting the mean amplitude of EPSCs in CA1 pyramidal neurons versus the stimulus intensities, we determined that the input-output curves were identical between genotypes (Figure 4E). The current-voltage (*I-V*) relations of AMPA receptor- and NMDA receptor-mediated EPSCs (EPSC<sub>SAMPA</sub>, Figure 4F, and EPSC<sub>NMDA</sub>, Figure 4G), and the induction of long-term potentiation (LTP, Figure 4H), also were not affected in the DAPK1<sup>-/-</sup> mice.

#### DAPK1 Activation Enhances Extrasynaptic NMDA Receptor Channel Activity

Having demonstrated that genetic deletion of DAPK1 did not alter NMDA receptor physiology, we next examined the functional impacts of DAPK1 deletion in NMDA receptor toxicity. First, we treated the cortical neurons from DAPK1<sup>-/-</sup> and DAPK1<sup>+/+</sup> mice with oxygen/glucose deprivation (OGD). Catalytic activity of DAPK1 was measured using immune-complex kinase assay with myosin light chain (MLC) as an endogenous substrate. We found that enzymatic activity of DAPK1 began to increase 5 min after OGD, and reached a peak 30 min later (Figure 5A). Activation of DAPK1 was maintained for over 30 min after OGD was washed out (Figures 5A and 5B). Activation of DAPK1 was not affected by applying AMPA receptor antagonist (10  $\mu$ M CNQX), but was completely eliminated either by applying NMDA receptor antagonist (50  $\mu$ M D-AP5) or by removing extracellular Ca<sup>2+</sup> (Ca<sup>2+</sup>-free, Figure 5C). Catalytic activity of DAPK1 is controlled by its autophosphorylation at serine-308 ( $pS^{308}$ ); dephosphorylation of  $pS^{308}$  allows DAPK1 to bind with CaM, thereby activating DAPK1 (Shohat et al., 2001). Consistent with this previous report, we found that DAPK1 became dephosphorylated at  $pS^{308}$  in cortical neurons following OGD exposure. Significantly, we showed that dephosphorylation of DAPK1 at  $pS^{308}$  was catalyzed by calcineurin (CaN, see also Figure S2).

Next, we investigated the functional impacts of an activated DAPK1 on NMDA receptor channels *in vivo*. We challenged the cortical neurons with OGD or with 50  $\mu$ M NMDA/10  $\mu$ M glycine for 30 min to activate an endogenous DAPK1. Western blots of the precipitates showed that the levels of  $pS^{1303}$ , but not the NR2B protein, were elevated in DAPK1<sup>+/+</sup> cortical neurons (Figure 5D). An increase of  $pS^{1303}$  in response to OGD (Figure 5D) or to NMDA challenging (Figures 5E and 5F) was not observed in DAPK1<sup>-/-</sup> neurons (Figure 5E). Thus, an activated DAPK1 is a response to phosphorylation of NR2B subunit at Ser-1303.

To determine whether an increase of the  $pS^{1303}$  level by an activated DAPK1 enhances synaptic NMDA receptor channel activity, we performed fluorescence ratio-metric Ca<sup>2+</sup> image combined with whole-cell patch clamp recordings. We found that Ca<sup>2+</sup> influx through synaptic NMDA receptor channels were not affected by an activated DAPK1; the peak amplitudes of Ca<sup>2+</sup> transients were identical between groups (Figure 5G). Since DAPK1 enhances the channel conductance of the recombinant NR1/NR2B receptors, which are known to be expressed predominantly in the extrasynaptic sites (Tovar and Westbrook, 1999; Brickley et al., 2003), we reasoned that an activated DAPK1 may functionally interact with extrasynaptic NMDA receptors. To test this possibility, we recorded the extrasynaptic NMDA receptor-mediated currents (eNMDAc) and Ca<sup>2+</sup> transients by blocking synaptic NMDA receptor channels using MK-801 trapping protocol (for details see Experimental Procedure). We treated the single cortical neurons with OGD or 50  $\mu$ M NMDA for 30 min to activate endogenous DAPK1. After a 30 min recovery period, the whole-cell currents and Ca<sup>2+</sup> transients were recorded (Figure 5H). A greater amplitude of eNMDAc and Ca<sup>2+</sup> transients was observed in DAPK1<sup>+/+</sup> neurons, compared to controls. Thus, an activated DAPK1 increases Ca<sup>2+</sup> influx through extrasynaptic NMDA receptor channels.

#### DAPK1 Deletion Protects against Cerebral Ischemic Neuronal Death

We next examined whether ischemic insult is mediated by DAPK1 induction of injurious Ca<sup>2+</sup> influx through extrasynaptic NMDA receptor channels. We challenged cortical cultures with OGD or 50  $\mu$ M NMDA/10  $\mu$ M glycine for 60 min. 24 hr after washout cell death was examined. Propidium iodide (PI) staining showed that genetic deletion of the DAPK1 gene sufficiently protected against the insults induced by either OGD or NMDA challenging (Figures 6A and 6B). Next, we subjected the DAPK1<sup>-/-</sup> and DAPK1<sup>+/+</sup> mice with transient global ischemia by occlusion of the common carotid artery for 20 min. Six days after reperfusion, brain sections were stained with Fluoro-Jade (FJ), a marker for degenerating neurons. An unbiased stereological analysis was used to count the FJ-labeled (FJ<sup>+</sup>) neurons in the CA1 area of the hippocampus, the layer 3 of the cortex, and the striatum. These three groups of neurons were examined because they are known to be vulnerable to transient global ischemic insult (Simon et al., 1984; Pellegrini-Giampietro et al., 1997; Wang et al., 2003a; Liu et al., 2004; Peng et al., 2006). In the DAPK1<sup>+/+</sup> mice, the majority of these neurons had degenerated (275  $\pm$  32 FJ<sup>+</sup> cells / 0.2 mm<sup>3</sup> in the cortex, 169  $\pm$  26 FJ<sup>+</sup> cells / 0.2 mm<sup>3</sup> in the striatum, and 361  $\pm$  38 FJ<sup>+</sup> cell/0.2 mm<sup>3</sup> in the CA1 region, n = 7 mice, Figures 6C–6E). This severe neuronal injury was observed only in the DAPK1<sup>+/+</sup> mice; markedly less damage was detected in the DAPK1<sup>-/-</sup> mice (81  $\pm$  14 FJ<sup>+</sup> cells / 0.2 mm<sup>3</sup> in the cortex, 59  $\pm$  9 FJ<sup>+</sup> cells / 0.2 mm<sup>3</sup> in the striatum, and 92  $\pm$  7 FJ<sup>+</sup> cell/0.2 mm<sup>3</sup> in the CA1 region, n = 6 mice, p < 0.01, Figure 6E). We also operated on mice to induce focal cerebral ischemia with middle cerebral artery occlusion (MCAO) for 60 min or 120 min. After 24 hr reperfusion, the brain infarction was analyzed using TTC staining. We found that the DAPK1<sup>-/-</sup> mice had a dramatic reduction of the brain infarction (14.2  $\pm$  2.1 mm<sup>3</sup> at 60 min MCAO; 29.6  $\pm$  3.3 mm<sup>3</sup> at 120 min

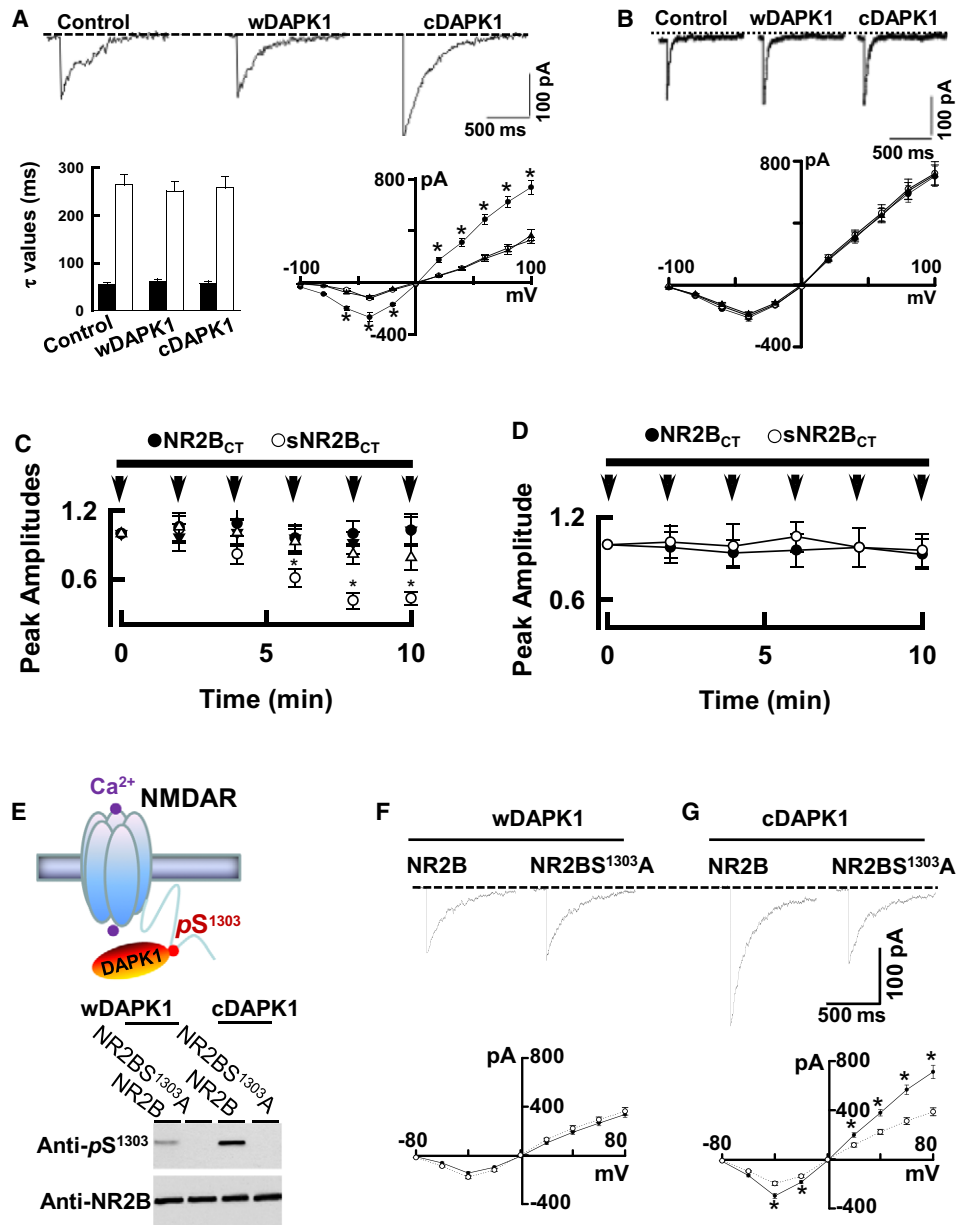


**Figure 3. DAPK1 Phosphorylates NR2B at Ser-1303 and Increase the Channel Conductance**

(A) Whole-cell currents at holding potential of  $-30$  mV in HEK293 cells coexpressing NR1/NR2B receptors without (control) or with wild-type DAPK1 (wDAPK1) or constitutively active DAPK1 (cDAPK1). Bar graph shows decay time constants of the receptor currents fitted with two exponential components with  $\tau_{fast}$  (75%, filled bars) and  $\tau_{slow}$  (25%, open bars). The peak currents were plotted against holding potentials without (open circles,  $n = 22$  cells) or with expression of wDAPK1 (triangles,  $n = 21$  cells) or cDAPK1 (filled circles,  $n = 22$  cells).

(B) Expression of cDAPK1 does not alter NR2A receptor currents. Whole-cell currents are at a holding potential of  $-60$  mV in HEK293 cells coexpressing the NR1/NR2A receptors without (control) or with wDAPK1 or cDAPK1. The peak currents were plotted against holding potentials without (open circles,  $n = 18$  cells) or with expression of wDAPK1 (filled circles,  $n = 18$  cells) or cDAPK1 (triangles,  $n = 18$  cells).

(C and D) NR2B<sub>CT</sub> antagonizes the cDAPK1-NR2B interaction. The averaged whole-cell currents are plotted against time with the intracellular perfusion of 10 (filled circles), 25 (open triangles) or 50  $\mu$ M NR2B<sub>CT</sub> (open circles) or 50  $\mu$ M sNR2B<sub>CT</sub> (filled triangles) in HEK293 cells coexpressing NR1/NR2B with cDAPK1 (C). In recordings from HEK293 cells coexpressing NR1/NR2B with wDAPK1 (D), 50  $\mu$ M NR2B<sub>CT</sub> (open circles) or sNR2B<sub>CT</sub> (filled circles) were applied. The peak currents were normalized to baseline (defined as 1.0,  $n = 22$  cell per group,  $*p < 0.01$ ). Horizontal above the graphs indicate the period of peptide administration. Arrows indicate the time of application of 1 ms pulse of 500  $\mu$ M glutamate.

(E) Illustration (top) shows that DAPK1 targets to NR2B C-terminal at Ser-1303. Bottom: the NR1/NR2B (lane: NR2B) or the mutant NR1/NR2B<sup>1303A</sup> (lane: NR2BS<sup>1303A</sup>) that were coexpressed with wDAPK1 or cDAPK1 in HEK293 cells were subjected to western blot with anti-pS<sup>1303</sup> or anti-NR2B. Similar results were observed in each of four experiments.

MCAO,  $n = 11$  mice/group), compared to DAPK1<sup>+/+</sup> mice ( $34.3 \pm 4.6$  mm<sup>3</sup> at 60 min MCAO;  $52.9 \pm 6.2$  mm<sup>3</sup> at 120 min MCAO;  $n = 11$  mice/group,  $p < 0.001$ , Figures 6F and 6G). This reduction of the brain infarction was associated with improvement of the neurological scores in DAPK1<sup>-/-</sup> mice ( $p < 0.01$ ,  $n = 11$  mice per group, Figure 6G). Thus, DAPK1 can be considered as a primary mediator in brain damage of stroke.

### Treatment of Stroke by Uncoupling DAPK1 from NMDA Receptor NR2B Subunit

DAPK1 physically and functionally interacts with the NMDA receptor NR2B subunit, and this interaction might act as an essential intracellular event in stroke damage. To investigate this, we examined whether blocking DAPK1-NR2B interaction achieves the therapeutic effects in mouse models with stroke. To do so, we generated cell membrane permeable NR2B<sub>CT</sub> peptide by fusing the NR2B<sub>CT</sub> to the cell-membrane transduction domain of the HIV-1 Tat protein (Tat-NR2B<sub>CT</sub>, for details see Experimental Procedures). Western blots of the precipitates revealed that application of Tat-NR2B<sub>CT</sub> sufficiently uncoupled an activated DAPK1 from the NMDA receptor NR2B subunit complex (Figure 7A). Although Tat-NR2B<sub>CT</sub> did not affect the catalytic activity of DAPK1 (Figure 7A), it completely blocked; [1]) an association between an activated DAPK1 and the NMDA receptor NR2B subunit; [2]) NR2B phosphorylation at Ser-1303 (Figure 7B, see also Figure S3); and [3]) Ca<sup>2+</sup> influx through NMDA receptor channels at extrasynaptic sites (Figure 7C).

We next operated on mice with MCAO for 60 min, and analyzed enzymatic activity of DAPK1. Our data revealed that DAPK1 in the forebrain of mice became activated 60 min, and reached a peak 120 min after reperfusion. Activation of DAPK1 was closely associated with phosphorylation of NR2B subunit at Ser-1303 (see also Figure S3). Blots of the anti-NR1 precipitates in the forebrain extracts showed Tat-NR2B<sub>CT</sub> at a dose of 10 mg/kg that did not alter the catalytic activity of DAPK1, but that sufficiently uncoupled an activated DAPK1 from NMDA receptor NR2B complex (see also Figure S3). By measuring the cerebral infarction 24 hr after MCAO operation using TTC staining, we found that the total infarction volume in the Tat-NR2B<sub>CT</sub>-treated mice was reduced to  $15.2 \pm 1.2$  mm<sup>3</sup>, compared to  $37.9 \pm 4.3$  mm<sup>3</sup> in control, in which mice were injected with Tat-sNR2B<sub>CT</sub> (mean  $\pm$  SEM,  $n = 11$  mice per group, ANOVA,  $F = 12.98$ ,  $p < 0.001$ , Figure 7D). Furthermore, a significant reduction of the cerebral infarction was also observed even when Tat-NR2B<sub>CT</sub> (10 mg/kg, *i.v.*) was administered 60 min after MCAO operation ( $19.3 \pm 1.9$  mm<sup>3</sup> in the Tat-NR2B<sub>CT</sub> post-treatment, and  $36.1 \pm 3.7$  mm<sup>3</sup> in Tat-sNR2B<sub>CT</sub>-post-treatment,  $n = 8$  mice/group, Figure 7D). A reduction of brain infarction was closely associated with improved neurological behaviors (Figure 7D). Together, our data demonstrate that DAPK1 physically and functionally interacts with the NMDA receptor NR2B subunit and that this interaction mediates stroke damage.

### DISCUSSION

NMDA receptor NR2B subunits have recently become the major focus of studies in the treatment of stroke because of their unique features (Hardingham et al., 2002; Simpkins et al., 2003; Liu et al., 2007). First, in the adult CNS neurons NMDA receptor NR2B subunits are localized predominantly at extra-synaptic sites (Tovar and Westbrook, 1999; Brickley et al., 2003). This feature enables the receptor to detect extrasynaptic glutamate spillover in the brain during ischemic insults (Drejer et al., 1985; Rossi et al., 2000). Second, extrasynaptic NMDA receptors are reported to link the specific signals that induce neuronal death in ischemia (Finkbeiner, 2000; Hardingham et al., 2002, Takasu et al., 2002; Liu et al., 2007). However, it is now believed that NMDA receptor NR2B subunits may be also combined with NR1/NR2A subunits to form NR1/NR2A/NR2B complex receptors at synapses (Thomas et al., 2006). Thus, using NMDA receptor NR2B subunit antagonists for selectively inhibiting extra-synaptic NMDA receptors still could be problematic.

Alternatively, recent studies have focused on NMDA receptor NR2B subunit downstream cell death signaling via interaction with PSD-95 (Aarts et al., 2002). Disturbing NR2B-PSD-95 interaction by expression of a peptide fragment of the NR2B C-terminal tail (KLSSIESDV) uncouples neuronal nitric synthase (nNOS) activation, protecting cerebral ischemic infarction in adult rats (Aarts et al., 2002). This finding suggests that blocking NR2B-PSD-95 interaction would be able to eliminate NMDA receptor NR2B subunit toxicity. However, this strategy has been challenged by its parallel inhibition of synaptic plasticity (El-Husseini et al., 2002). Also, some other studies indicated that inhibition of PSD-95 increased brain damage in stroke (Gardoni et al., 2002).

Multiple intracellular signals are able to regulate NMDA receptor channel activity (Ghosh, 2002) and induce NMDA receptor-dependent cell death (Simon et al., 1984; Wang et al., 1999). Some including calcineurin (CaN) (Wang et al., 1999), Ca<sup>2+</sup>/CaM-activated protein kinase II (CaMK-II) (Mabuchi et al., 2001), protein kinase C (Sun et al., 2008), cyclin-dependent kinase 5 (Cdk5) (Wang et al., 2003a), tyrosine kinases (Khanna et al., 2007), and nNOS (Eliasson et al., 1999), however, also control the physiological processes of gene expression, as well as synaptic plasticity (Ghosh, 2002; Salter and Kalia, 2004), and thus are not promising targets for stroke therapy.

DAPK1 belongs to a Ca<sup>2+</sup>/CaM-dependent protein kinase family, and comprises a kinase domain, a CaM-binding motif, eight ankyrin repeats, and a death domain (for reviews, see Bialik and Kimchi, 2006; Van Eldik, 2002; Velentza et al., 2001). The kinase domain resides at the amino terminus and precedes the CaM-binding motif, which consists of a CaM binding site and an autoinhibitory region. CaM binding to the CaM binding site induces a conformation change. This conformation change is known to relieve the steric block of the active site by the autoinhibitory region (Van Eldik, 2002), and possibly leads to an

(F and G) Whole-cell currents are recorded at holding potential of  $-30$  mV in HEK293 cells coexpressing NR1/NR2B or the mutant NR1/NR2BS<sup>1303A</sup> receptors with wDAPK1(F) or cDAPK1 (G). The peak currents were plotted against holding potentials in HEK293 cells with expression of NR1/NR2B (filled circles,  $n = 23$  cells) or the mutant NR1/NR2BS<sup>1303A</sup> (open circles,  $n = 21$  cells). In panels A–G, data are mean  $\pm$  SEM, \* $p < 0.01$ .

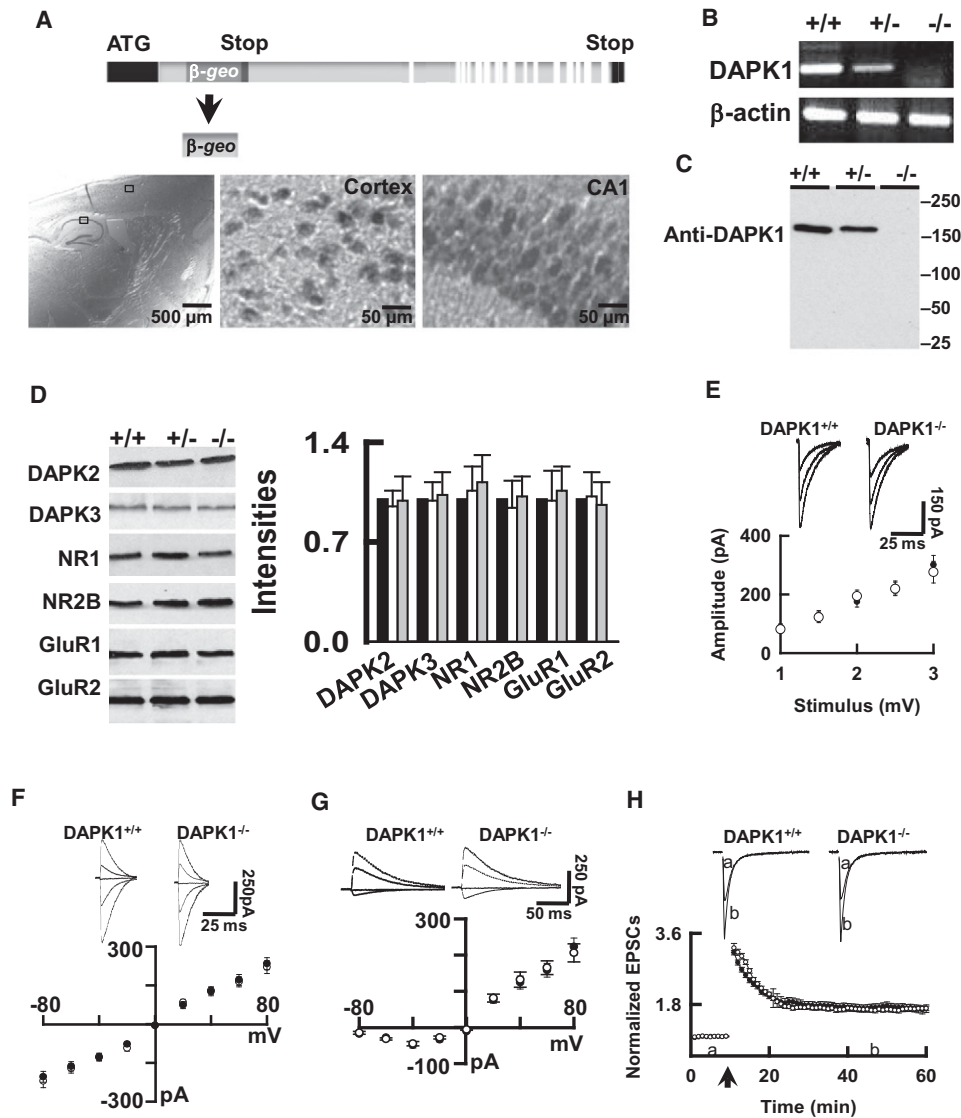


**Figure 4. The Mutant Mice Lacking the DAPK1 Gene Have Normal Synaptic Transmission**

(A) A promoterless gene trapping vector fused into a reporter gene ( $\beta$ -geo) was inserted into the first intron of DAPK1. Staining on a sagittal brain section from an adult DAPK1<sup>-/-</sup> mouse shows the  $\beta$ -geo protein in the cortex and hippocampus.

(B and C) Representatives show the RT-PCR and western blots of DAPK1 mRNA (B) and proteins (C) in the brain of the homozygous (DAPK1<sup>-/-</sup>), heterozygous (DAPK1<sup>+/-</sup>) and their wild-type littermates (DAPK1<sup>+/+</sup>) mice.

(D) Blots show DAPK2, DAPK3, and synaptic proteins in the brains of DAPK1<sup>+/+</sup>, DAPK1<sup>+/-</sup>, and DAPK1<sup>-/-</sup> mice. The intensities of the blots (bar graph) were normalized to the respective blots in DAPK1<sup>+/+</sup> mice (defined as 1.0). Data are mean  $\pm$  SEM (n = 4 mice/group).

(E) The DAPK1<sup>-/-</sup> mice have normal input-output responses. The EPSCs (top) were recorded from CA1 pyramidal neurons at holding potential of -70 mV. The mean amplitudes from DAPK1<sup>+/+</sup> (open circles) and DAPK1<sup>-/-</sup> (filled circles) mice, as summarized in graph (bottom), were plotted against the intensities of stimulus. Data are mean  $\pm$  SEM (n = 8 cells/4 mice per group).

(F and H) Sweeps (top) and the current-voltage relations of the excitatory post-synaptic currents (EPSCs) mediated by AMPA (EPSCs<sub>AMPA</sub>, F) and the NMDA receptors (EPSCs<sub>NMDA</sub>, G) at holding potentials of -80, -40, 0 +20, or +40 mV were recorded in CA1 neurons from DAPK1<sup>+/+</sup> (open circles) and DAPK1<sup>-/-</sup> (filled circles) mice. Data are mean  $\pm$  SEM (n = 12 cells/6 mice per group).

(H) A plot represents the normalized peak amplitude of the EPSCs<sub>AMPA</sub> in CA1 neurons from DAPK1<sup>+/+</sup> (open circles) and DAPK1<sup>-/-</sup> mice (filled circles). The traces above the graph are averages of three sweeps taken at the time points indicated by the letter above the x axis. Arrow indicates the time of tetanus. Data are mean  $\pm$  SEM (n = 12 cell/6 mice per group).

activated DAPK1 binding with the NMDA receptor NR2B subunit. Consistent with this idea, our data revealed that activation of DAPK1 following ischemic insult phosphorylates the

NMDA receptor NR2B subunit at Ser-1303. Interestingly, the NR2B at Ser-1303 is the same residue as that catalyzed by CaMK-II (Omkumar et al., 1996). Thus, DAPK1 may have

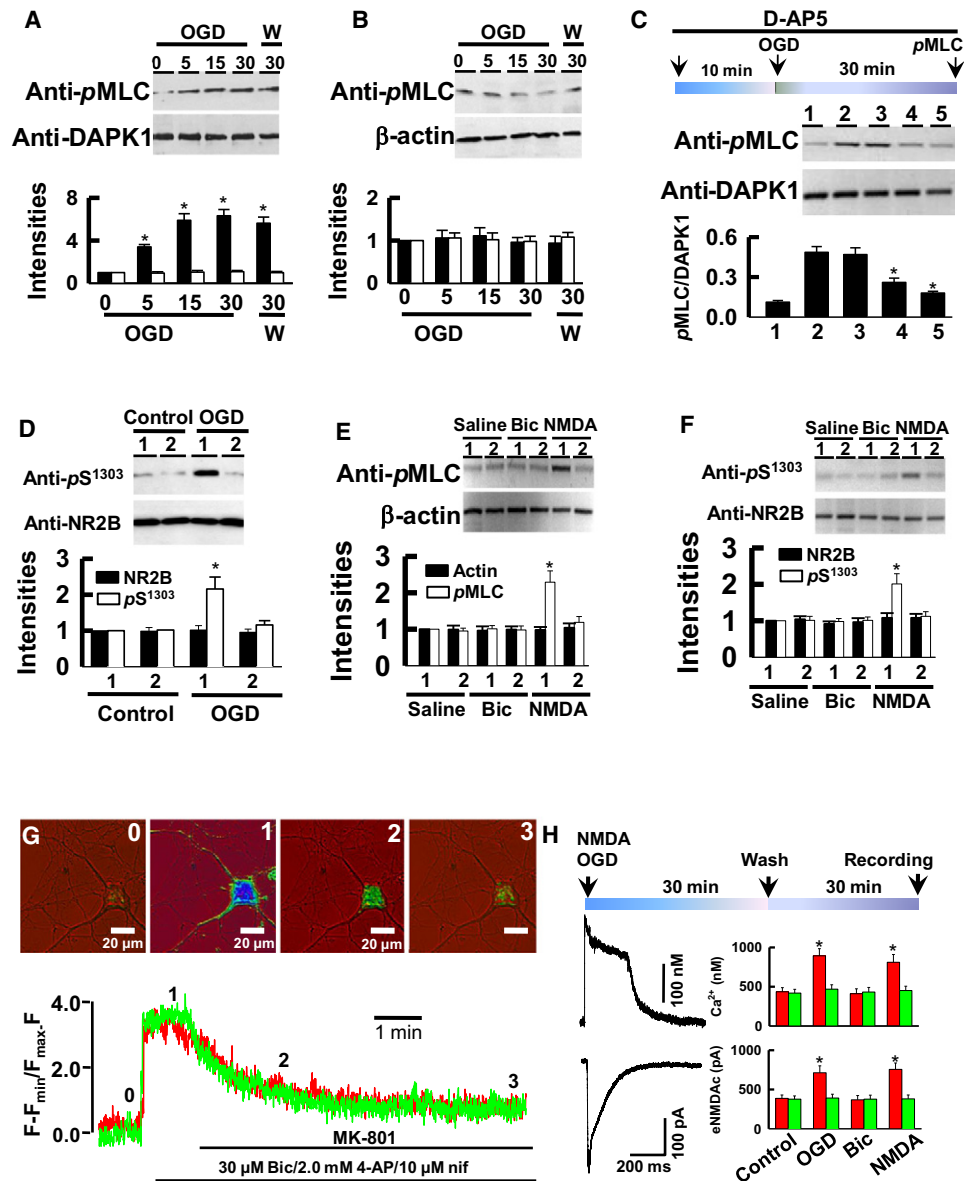


### Figure 5. Activation of DAPK1 Induces Ca<sup>2+</sup> Influx through Extrasynaptic NMDA Receptors

(A and B) DAPK1<sup>+/+</sup> (A) and DAPK1<sup>-/-</sup> (B) cortical neurons were exposed to OGD for 0, 5, 15, or 30 min. Immediately after OGD (OGD) or 30 min after OGD washout (w), DAPK1 complex was precipitated and blotted with anti-pMLC or anti-DAPK1. The intensities of the anti-pMLC (filled bars) and anti-DAPK1 (open bars) blots were normalized to their respective signals at 0 min OGD (defined as 1.0, n = 16).

(C) DAPK1<sup>+/+</sup> neurons were treated with saline (lane 1 and lane 2), 10  $\mu$ M CNQX (lane 3), 50  $\mu$ M D-AP5 (lane 4), or Ca<sup>2+</sup>-free (lane 5) for 10 min, and then challenged with sham control (lane 1) or with OGD (lane 2 through lane 5) for 30 min. DAPK1 complex was then precipitated and blotted with anti-pMLC or anti-DAPK1. The ratio of anti-pMLC versus anti-DAPK1 blots were calculated (n = 12 cultures/4 mice) and summarized in bar graph.

(D) DAPK1<sup>+/+</sup> (lane 1) and DAPK1<sup>-/-</sup> (lane 2) neurons were exposed to saline or OGD for 30 min. NMDA receptor complex was precipitated with anti-NR1 and blotted with anti-pS<sup>1303</sup> or anti-NR2B. The intensities of blots were normalized to their respective controls (defined as 1.0, n = 12 cultures/4 mice).

(E and F) NMDA treatment activates DAPK1 (E) and increases the levels of pS<sup>1303</sup> in cortical neurons (F). DAPK1<sup>+/+</sup> (lane 1) and DAPK1<sup>-/-</sup> (lane 2) cortical neurons were challenged with saline, 10  $\mu$ M bicuculline (Bic), or 50  $\mu$ M NMDA/10  $\mu$ M glycine for 30 min. Endogenous DAPK1 and NMDA receptor protein complexes were then precipitated and blotted, as indicated. The intensities of the blots were normalized to their respective controls (defined as 1.0), and summarized in bar graphs (n = 12 cultures/4 mice).

(G) Images are taken at the time points indicated by the numbers above the traces from single DAPK1<sup>+/+</sup> neuron with pre-OGD (Red) or sham (Green). Ca<sup>2+</sup> transients were evoked by 30  $\mu$ M Bic and 10  $\mu$ M nifedipine (Nif) and blocked by 10  $\mu$ M MK-801.

(H) Cortical neurons were exposed to control, OGD, 10  $\mu$ M Bic, or 50  $\mu$ M NMDA/10  $\mu$ M glycine for 30 min. 30 min after washout Ca<sup>2+</sup> transients and whole-cell currents (eNMDAc) were evoked by a 5-ms pulse of 100  $\mu$ M NMDA/10  $\mu$ M glycine. Data (\*p < 0.01) in bar graphs are DAPK1<sup>+/+</sup> (red bars) and DAPK1<sup>-/-</sup> (green bars) neurons (n = 22 cells per group).

In panels A–H, data in bar graphs are mean  $\pm$  SEM. See also Figure S2.

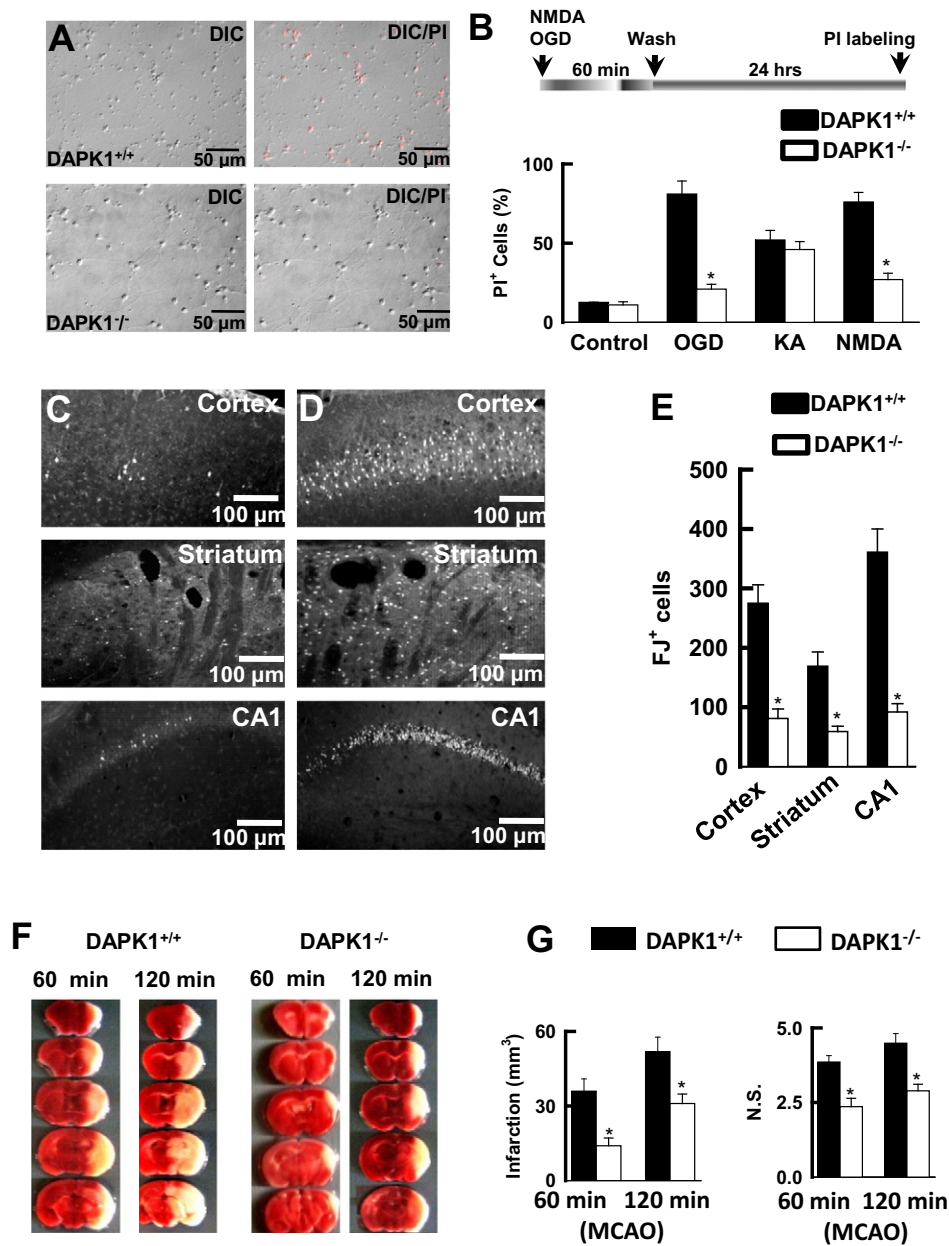


**Figure 6. Genetic Deletion of DAPK1 Protects against Ischemic Neuronal Death**

(A) DAPK1 deletion protects cortical neurons against OGD insult. DAPK1<sup>+/+</sup> and DAPK1<sup>-/-</sup> cortical cells were challenged with OGD for 60 min. 24 hr after washout the cultures were stained with propidium iodide (PI, red), and single DIC or double DIC/PI images were collected. (B) Bar graph summarizes the percentage of PI<sup>+</sup> cells (n = 12 cultures). Data are mean ± SEM. (C–E) Images of cortex, striatum and the hippocampus from DAPK1<sup>-/-</sup> (C) and DAPK1<sup>+/+</sup> (D) mice that were stained with Fluoro-Jade 6 days after transient global ischemia. Bar graph (E) shows summarized Fluoro-Jade-labeled cells (n = 7). Data are mean ± SEM. (F and G) Images of the brain sections (1.0 mm, F) from DAPK1<sup>+/+</sup> and DAPK1<sup>-/-</sup> mice 24 hr after operation for 60 min or 120 min MCAO that were stained with TTC. Bar graphs show the infarct volume and neurological scores (N.S.). Data are mean ± SEM (\*p < 0.01).

a functional analogous to that of CaMK-II. CaMK-II is one of the most abundant Ca<sup>2+</sup>/CaM-dependent enzymes in the central neurons and participates in synaptic plasticity (Lisman et al., 2002) as well as in the cellular events responsible for ischemic neuronal death (Waxham et al., 1996). However, CaMK-II was

found to become inactivated in the brain in response to ischemic insults (Hanson et al., 1994; Waxham et al., 1996; Petersen et al., 2003). Inhibition of CaMK-II enhances the vulnerability of brain cells to stroke damage (Waxham et al., 1996). In this context, CaMK-II can be viewed as a neuronal survival mediator. Thus,

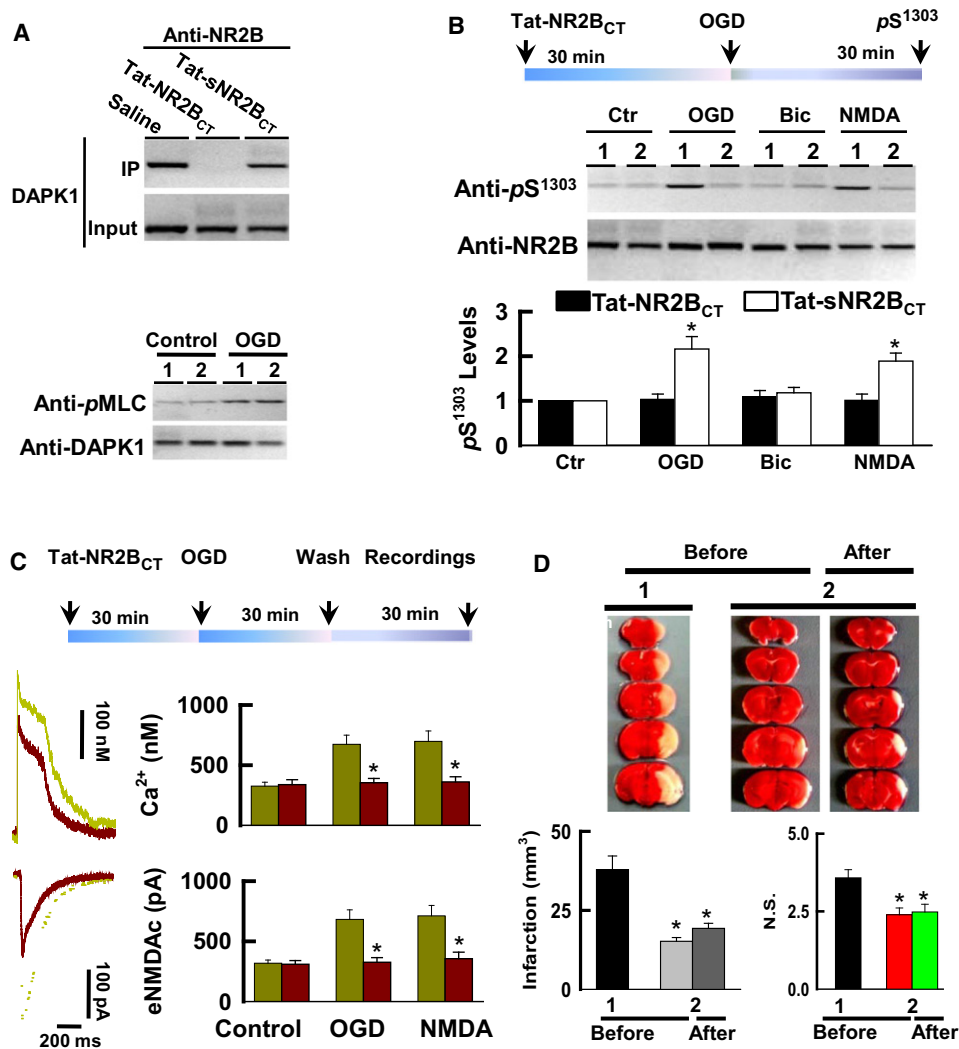


**Figure 7. Inhibition of DAPK1-NMDA Receptor Interaction Protects against Stroke Damage**

(A) Tat-NR2B<sub>CT</sub> treatment disturbs the DAPK1-NMDA receptor association without affecting DAPK1 activity. DAPK1<sup>+/+</sup> cortical neurons were treated with 50  $\mu$ M Tat-NR2B<sub>CT</sub> or Tat-sNR2B<sub>CT</sub> or saline for 30 min and exposed to OGD for 30 min. NMDA receptor complex was precipitated with anti-NR2B (top) or anti-DAPK1 (bottom) and blotted with anti-DAPK1 or anti-pMLC, as indicated.

(B) DAPK1<sup>+/+</sup> cortical neurons were treated with 50  $\mu$ M Tat-sNR2B<sub>CT</sub> (lane 1) or Tat-NR2B<sub>CT</sub> (lane 2) for 30 min and were then exposed to control, OGD, 10  $\mu$ M bicuculline (Bic), or 50  $\mu$ M NMDA/10  $\mu$ M glycine for 30 min. Anti-NR1 precipitates were blotted with anti-pS<sup>1303</sup> or anti-NR2B, as indicated. Data in bar graph are mean  $\pm$  SEM (n = 16 cultures/4 mice, \*p < 0.01).

(C) DAPK1<sup>+/+</sup> cortical neurons were treated with 50  $\mu$ M Tat-sNR2B<sub>CT</sub> (purple traces) or Tat-NR2B<sub>CT</sub> (green traces) for 30 min and were then exposed to control, OGD or 50  $\mu$ M NMDA/10  $\mu$ M glycine for 30 min. 30 min after washout and Ca<sup>2+</sup> transients (top traces) whole-cell currents (bottom traces) were recorded. Data from Tat-NR2B<sub>CT</sub> (purple bars) and Tat-sNR2B<sub>CT</sub> (green bars) in bar graphs are mean  $\pm$  SEM (n = 16 recordings per group, \*p < 0.01).

(D) The adult male DAPK1<sup>+/+</sup> mice were received a single injection (10 mg/kg, i.v.) of Tat-NR2B<sub>CT</sub> (1) or Tat-sNR2B<sub>CT</sub> (2) 60 min before or 60 min after MCAO (After). The infarction volume and neurological scores (N.S.) were summarized in the bar graphs (G). Data are mean  $\pm$  SEM (\*p < 0.001).

See also Figure S3.

it is unlikely that CaMK-II plays a role in the DAPK1-NR2B interaction for ischemic neuronal death.

In the present study, we used Tat-NR2B<sub>CT</sub> to disrupt the interaction between an activated DAPK1 and NMDA receptor NR2B. Tat-NR2B<sub>CT</sub>, but not its scrambled control, protected cortical neurons from NMDA receptor-mediated insults without affecting catalytic activity of DAPK1 or the NMDA receptor physiology. Thus, systematic administration of Tat-NR2B<sub>CT</sub> could serve as

an advantage over NMDA receptor antagonists in stroke therapy. Indeed, our data demonstrated that Tat-NR2B<sub>CT</sub>, even when it was administered one hour after stroke onset, dramatically reduced brain infarction and improved neurological functions in mice. Thus, targeting the interaction between an activated DAPK1 and NMDA receptor NR2B could be considered a promising strategy for the treatment of stroke. It must be noted, however, that even though we found that Tat-NR2B<sub>CT</sub> disrupted

DAPK1-NR2B interaction without interfering with the association of NR2B with PSD-95 or CaMK-II, we could not exclude the possibility that inhibition of other binding proteins, rather than DAPK1 interaction with NMDA receptor NR2B by Tat-NR2B<sub>CT</sub>, could be responsible for its neuronal protective effects.

A main question arising from this study is how DAPK1 becomes activated in response to cerebral ischemic insults. Catalytic activity of DAPK1 is thought to be controlled by its autophosphorylation at serine-308 ( $pS^{308}$ ); dephosphorylation of  $pS^{308}$  allows DAPK1 to bind with CaM, thereby activating DAPK1 (Shohat et al., 2001). In the present study, we showed that DAPK1 becomes dephosphorylated at  $pS^{308}$  in cortical neurons following ischemic insults (Figure S2). We also demonstrated that dephosphorylation of  $pS^{308}$  in response to ischemic insults can be eliminated by genetic mutation of calcineurin (CaN, see also Figure S2). Thus, CaN can be considered as an upstream activator of DAPK1. It has been known that enzymatic activity of CaN depends on  $Ca^{2+}$  influx through NMDA receptor channels (Marshall et al., 2003). Consistent with this previous report, our data revealed that challenging cortical neurons with NMDA induced dephosphorylation of  $pS^{308}$  (Figures 5C–5E). Conversely, application of NMDA receptor antagonist or removal of extracellular  $Ca^{2+}$  inhibits DAPK1 dephosphorylation at  $pS^{308}$  and inactivates DAPK1 (Figure 5C, see also Figure S2). Thus, the most parsimonious explanation for our findings is that under physiological conditions, an initial  $Ca^{2+}$  influx through NMDA receptor channels produces partial inhibition of NMDA receptors via  $Ca^{2+}$ -dependent inactivation, thereby preventing the intracellular  $Ca^{2+}$  overloading (Krupp et al., 1999). Under pathological conditions such as ischemic insults, however,  $Ca^{2+}$  influx through NMDA receptor channels activates CaN and in turn dephosphorylates DAPK1 at  $pS^{308}$ , leading to activation of DAPK1. An activated DAPK1 is recruited into the NMDA receptor NR2B subunit at extrasynaptic sites and phosphorylates NR2B subunit at Ser-1303 and subsequently induces injurious  $Ca^{2+}$  influx through NMDA receptor channels, resulting in an irreversible neuronal death. Thus, DAPK1 can be considered as a signaling amplifier of NMDA receptors at extrasynaptic sites for mediating brain damage in stroke.

## EXPERIMENTAL PROCEDURES

### Generation of DAPK1 Null Mutant Mice

The null mutant mice with complete deletion of DAPK1 gene were generated using a gene-trapping technique. A mouse (strain C57/Bl6) was cloned from an embryonic stem cell line (IST12766D5; Texas Institute for Genomic Medicine, TIGM), carrying DAPK1 allele disrupted by the insertion of a gene trap vector with a lacZ ( $\beta$ -galactosidase)-neomycin resistance fusion cassette ( $\beta$ -gal, Omnibank Vector 76) in the first intron. The insertion site, as denoted with an asterisk\*, was confirmed by genomic sequence, which is available upon requested. The cloned ES cell was used to generate DAPK1 mutant mice with a C57/Bl6 background, which were verified by PCR amplification of the mutant gene in tail DNA from progeny. The homozygous (DAPK1<sup>-/-</sup>) mice were derived by mating heterozygous DAPK1<sup>+/-</sup> mice. The PCR primers for wild DAPK1 were as follows: sense 5'TTGACACAACAGCTACACAGC-3' antisense 5' ATAGTCCCCTACTCAGGTC-3'.

### Focal Cerebral Ischemia and Transient Global Ischemia

DAPK1 mutant mice were fasted overnight, and anesthetized with 4% halothane and maintained with mechanical ventilation (3.5 ml/cycle, 28 cycle/min,

0.5% halothane in a mixture of 30% O<sub>2</sub> and 70% N<sub>2</sub>O). The blood gas conditions were kept at constant levels throughout the surgery (P<sub>O<sub>2</sub></sub>, 120 ± 10 mm Hg; P<sub>CO<sub>2</sub></sub>, 35 ± 3 mm Hg), and the rectal and temporal muscle temperatures were also maintained at 37.5 ± 0.2°C and 37.0 ± 0.1°C, respectively. Body temperature was maintained at 37 ± 0.5°C with heating pads until the animals had recovered from surgery. Focal cerebral ischemia was induced by intraluminal middle cerebral artery occlusion (MCAO), as described previously. Local blood flow was monitored using BLF21C Laser Doppler Flow-meter with LL-M1043 fiber flow-probe (Transonic System Inc, New York), as described before (Wang et al., 2003a; Liu et al., 2004; Peng et al., 2006, see also Extended Experimental Procedures).

### Administration of Tat-NR2B<sub>CT</sub>

Mice were intravenously (i.v.) administered with 10 mg/kg Tat-NR2B<sub>CT</sub> (Tat-KKNNRNLRRQHSY) or Tat-sNR2B<sub>CT</sub> (Tat-NRRNRNSKLQHKKY) 60 min before or after MCAO operation. To test whether the Tat-peptide could be delivered into the brain, the Tat-NR2B<sub>CT</sub>-fluorescein isothiocyanate (FITC, 10 mg/kg, i.v.) was injected. 30 min after the injection, the brain sections (30  $\mu$ m) were imaged under the Axio Observer 200 Apotome microscope (data not shown). For the electrophysiological recordings, 50  $\mu$ M NR2B<sub>CT</sub> or sNR2B<sub>CT</sub> was applied directly into the recording cells via patch electrode. A dose of 10 mg/kg tat peptide or 50  $\mu$ M NR2B<sub>CT</sub> peptide was chosen because we found they did not alter DAPK1 activity but uncoupled an activated DAPK1 from NMDA receptor complex. The peptides with 99% purity were synthesized by AnaSpec (San Jose, CA) and Peptide 2.0, Inc (Chantilly, VA), respectively. The peptides were numbered and the experimenters were unaware of which one was applied in all experiments.

### Whole-Cell Patch Clamp Recordings

Hippocampal slices (300  $\mu$ m) were prepared from mice as previously described (Wang et al., 2003a; 2003b; Liu et al., 2004; Peng et al., 2006, see also Extended Experimental Procedures). Slices in the recording chamber were continuously superfused with artificial cerebrospinal fluid (ACSF, 2 ml/min) saturated with 95% O<sub>2</sub>/5% CO<sub>2</sub> at 30 ± 1°C. The composition of ACSF (in mM) was 124 NaCl, 3 KCl, 1.25 NaH<sub>2</sub>PO<sub>4</sub>, 1.2 MgCl<sub>2</sub>, 2 CaCl<sub>2</sub>, 26 NaHCO<sub>3</sub>, and 10 dextrose.

### Co-IP, Affinity Binding Assay, and Western Blots

Cerebral cortex was homogenized in ice-cold lysis buffer containing (mM) 50 Tris-HCl, 150 NaCl, 1% NP-40, 2 EDTA, 1 Na-orthovanadate, (pH 7.4), and proteinase inhibitor mixture (Sigma, 5  $\mu$ l/100 mg tissue). After clearing debris by centrifuging at 14,000  $\times$  g at 4°C, protein concentration in the extracts was determined by Bradford assay (Bio-Rad, Hercules, CA). The extracts (~500  $\mu$ g protein) were incubated with nonspecific IgG (2  $\mu$ g) or polyclonal rabbit anti-NR2B (2  $\mu$ g; Millipore) or anti-DAPK1 (2  $\mu$ g, Sigma) overnight at 4°C, followed by the addition of 40  $\mu$ l of Protein G-Sepharose (Sigma) for 3 hr at 4°C. The precipitates were washed four times with lysis buffer and denatured with SDS sample buffer and separated by 12% SDS-PAGE. Proteins were transferred onto nitrocellulose membranes using a Bio-Rad mini-protein-III wet transfer unit overnight at 4°C. Transfer membranes were then incubated with blocking solution [5% nonfat dried milk dissolved in TBST buffer containing (mM); 10 Tris-HCl, 150 NaCl, and 0.1% Tween-20 for 1 hr at room temperature, washed three times, and incubated with anti-goat primary antibody against NR1 (1:1000, Santa Cruz), anti-rabbit antibody against NR2A (anti-NR2A, 1:1000; Millipore), NR2B (anti-NR2B, 1:1000; Millipore), PSD-95 (anti-PSD-95, 1:1000; Santa Cruz), or anti-DAPK1 (1: 1000, Sigma) for 1 hr at room temperature. Membranes were washed three times with TBST buffer and incubated with the appropriate secondary antibodies (1:1000 dilution) for 1 hr followed by washing four times. Signal detection was performed with an enhanced chemiluminescence kit (Amersham Biosciences, Arlington, IL). The lanes marked "input" were loaded with 10% of the starting material used for immunoprecipitation.

To determine direct binding of DAPK1 with NMDA receptor NR2B C-terminal domain, the GST-NR2B deletion mutants (GST-NR2B<sup>839-1482</sup>, GST-NR2B<sup>839-1261</sup>, GST-NR2B<sup>1261-1292</sup>, GST-NR2B<sup>1292-1304</sup>, and GST-NR2B<sup>1305-1482</sup>) were generated and purified. Purified GST fusion proteins were separated on SDS-PAGE and transferred onto a nitrocellulose

membrane, which was washed with distilled water and blocked with TBST for 1 hr at room temperature. The membrane was then incubated with affinity binding buffer containing 50 mM Tris-HCl, (pH 7.5), 200 mM NaCl, 12 mM  $\beta$ -mercaptoethanol, 1.0% polyethylene glycol, 10  $\mu$ g/ml protease inhibitors and 500  $\mu$ g/ml purified flag-tagged DAPK1 (Invitrogen) for 1 hr at room temperature and washed four times for 5 min with affinity binding buffer. Bound DAPK1 was detected with anti-Flag (1: 2000, Invitrogen).

### Protein Identification

Protein bands were excised manually from the Coomassie blue-stained gels and then digested automatically using a Proteomeer DP protein digestion station (Bruker-Daltonics, Bremen, Germany). Tryptic products were analyzed using Nano-Liquid Chromatography-Tandem Mass Spectrometry (NLC/MS). Each spectrum was internally calibrated with mass signals of trypsin autolysis ions to reach a typical mass measurement accuracy of  $\pm$  10 ppm. Raw data were searched in the SWISS-PROT database.

### Cell Cultures and Oxygen-Glucose Deprivation

Hippocampi were isolated from the E20 DAPK1 mice. Cells were dissociated and purified using papain dissociation kit (Worthington Biochemical Corporation) plated with the densities of 100–150 cells/mm for  $\text{Ca}^{2+}$  image or 800–1000 cells/mm for OGD on 19 mm coverslips coated with 30  $\mu$ g/ml poly-D-lysine and 2  $\mu$ g/ml laminin. Cells were placed in fresh serum-free Neurobasal Medium (21103, GIBCO) plus 2% B27 and fed every 4 days with fresh media and used after 18 days (DIV18). Oxygen/glucose deprivation (OGD) was induced by perfusion (2 ml/min) of a glucose-free bicarbonate-buffer containing (in mM) 120 NaCl, 5 KCl, 2.0  $\text{CaCl}_2$ , 0.8  $\text{MgCl}_2$ , 25  $\text{NaHCO}_3$ , (pH 7.4), at 32°C, saturated with 5%  $\text{CO}_2$ /10%  $\text{H}_2$ /85% $\text{N}_2$  for 0, 5, 15, or 30 min. Zero or 30 min after OGD washout, the cultures were used for enzymatic assays. In all NMDA treatment, 10  $\mu$ M glycine was included. The phosphorylated myosine light chain (MLC) at Thr-18 and Ser-18 (pMLC) that was catalyzed by an activated DAPK1 in the lysates was blotted with anti-pMLC (1:1000, Millipore) or anti-pDAPK1 (1:500, Millipore) that specifically recognizes the phosphorylated DAPK1 at Ser-308. For measurement of phosphorylation of the NMDA receptor NR2B subunit at Ser-1303 (pS<sup>1303</sup>), the NMDA receptor complex was immunoprecipitated using anti-NR1. The precipitates were then probed using anti-pS<sup>1303</sup> (1:1000, anti-phospho-NR2B at Ser1303 with antigen: RRQHPsYDTF, Millipore). The bands were quantified using “the normalized method” of the densitometer Quantity One following the Quantity One user instructions (Bio-Rad). The intensities of the bands marked “0” in each gel were normalized as 1. Each of the other bands in the same gel was then normalized to “0” bands.

### $\text{Ca}^{2+}$ Imaging

For  $\text{Ca}^{2+}$  imaging, the neuronal cultures were loaded with fura-2-AM (1  $\mu$ M, Invitrogen) for 30 min followed by 5 washes for 30 min. The cultures were then subjected to OGD for 30 min (OGD, pre-OGD-treated) or 0 min (control). The 30 min OGD was chosen because it activates DAPK1 without causing morphological changes, thereby ensuring accurate measurement of  $\text{Ca}^{2+}$  signals in single neurons. Immediately after OGD washout, the cultures were perfused at 4 ml/min with a glucose-containing bicarbonate buffer 135 NaCl, 5 KCl, 2.0  $\text{CaCl}_2$ , 25  $\text{NaHCO}_3$ , and 10 glucose, (pH 7.4), at 32°C, saturated with 5%  $\text{CO}_2$ /10%  $\text{H}_2$ /85% $\text{O}_2$ . Synaptic NMDA receptors were activated by applying 30  $\mu$ M bicuculline (Bic)/2 mM 4-AP in the presence of 10  $\mu$ M nifedipine. One min after Bic/4-AP, MK-801 (20  $\mu$ M, Sigma) was applied for blocking synaptic NMDA receptor channels. Since MK-801 is an irreversible open channel blocker, activated synaptic NMDA receptor channels remained blocked after MK-801 washout. To ensure these synaptic NMDA receptor channels were not reactivated, we applied AMPA receptor antagonist CNQX (10  $\mu$ M) to block neuronal spontaneous firing. The extrasynaptic NMDA receptors were activated by a 5 ms pulse of 100  $\mu$ M NMDA/10  $\mu$ M glycine (Sigma) in the presence of 10  $\mu$ M CNQX (Tocris) and 10  $\mu$ M nifedipine (Sigma). One min later 10  $\mu$ M ifenprodil was applied using SmartSquirt 4-Micro-Perfusion System with ValveLink8.2 controller (AutoMate Scientific, Berkeley, CA). Fura-2 340 and 380 nm fluorescence imaging pairs were collected through an AxioCam MRM REV3 camera, which was equipped with an Axio Observer 200 microscope with a 63  $\times$  Fluor water immersion objective. The images were

captured with 30 cycles/second using Axiovision 4.7 software in Carl Zeiss Imaging Station 35A with XP Pro. Calcium concentrations were expressed as a function of the  $[\text{Ca}^{2+}]/K_d = [(F-F_{\text{min}})/(F_{\text{max}}-F)]$ . The average values that were normalized to basal line (defined as 1.0) were determined for each 20 s period of measurement (60 images).

### SUPPLEMENTAL INFORMATION

Supplemental Information includes Extended Experimental Procedures, three figures, and two tables and can be found with this article online at doi:10.1016/j.cell.2009.12.055.

### ACKNOWLEDGMENTS

This work was supported by the American Heart Association (05553413YL; 0535201YC; and 0625532 XZ), National Institute of Health (NIH/NINDS, R01NS051383YL and NIH/NIA R01AG033282YL). We thank Ryan Labadens at the Neuroscience Center of Excellence, Louisiana State University School of Medicine Health Sciences Center, and for assistance in manuscript preparation and discussion.

Received: December 12, 2008

Revised: October 16, 2009

Accepted: December 29, 2009

Published: January 21, 2010

### REFERENCES

- Aarts, M., Liu, Y., Liu, L., Besshoh, S., Arundine, M., Gurd, J.W., Wang, Y.T., Salter, M.W., and Tymianski, M. (2002). Treatment of ischemic brain damage by perturbing NMDA receptor- PSD-95 protein interactions. *Science* 298, 846–850.
- Aarts, M., Iihara, K., Wei, W.L., Xiong, Z.G., Arundine, M., Cerwinski, W., MacDonald, J.F., and Tymianski, M. (2003). A key role for TRPM7 channels in anoxic neuronal death. *Cell* 115, 863–877.
- Bano, D., Young, K.W., Guerin, C.J., Lefevre, R., Rothwell, N.J., Naldini, L., Rizzuto, R., Carafoli, E., and Nicotera, P. (2005). Cleavage of the plasma membrane  $\text{Na}^+/\text{Ca}^{2+}$  exchanger in excitotoxicity. *Cell* 120, 275–285.
- Bialik, S., and Kimchi, A. (2006). The Death-Associated Protein Kinases: Structure, Function, and Beyond. *Annu. Rev. Biochem.* 75, 189–200.
- Brickley, S.G., Misra, C., Mok, M.H., Mishina, M., and Cull-Candy, S.G. (2003). NR2B and NR2D subunits coassemble in cerebellar Golgi cells to form a distinct NMDA receptor subtype restricted to extrasynaptic sites. *J. Neurosci.* 23, 4958–4966.
- Chatterton, J.E., Awobuluyi, M., Premkumar, L.S., Takahashi, H., Talantova, M., Shin, Y., Cui, J., Tu, S., Sevarino, K.A., Nakanishi, N., et al. (2002). Excitatory glycine receptors containing the NR3 family of NMDA receptor subunits. *Nature* 415, 793–798.
- Drejer, J., Benveniste, H., Diemer, N.H., and Schousboe, A. (1985). Cellular origin of ischemia-induced glutamate release from brain tissue in vivo and in vitro. *J. Neurochem.* 45, 145–151.
- Eliasson, M.J., Huang, Z., Ferrante, R.J., Sasamata, M., Molliver, M.E., Snyder, S.H., and Moskowitz, M.A. (1999). Neuronal nitric oxide synthase activation and peroxynitrite formation in ischemic stroke linked to neural damage. *J. Neurosci.* 19, 5910–5918.
- El-Husseini, Ael-D., Schnell, E., Dakoji, S., Sweeney, N., Zhou, Q., Prange, O., Gauthier-Campbell, C., Aguilera-Moreno, A., Nicoll, R.A., and Brecht, D.S. (2002). Synaptic strength regulated by palmitate cycling on PSD-95. *Cell* 108, 849–863.
- Finkbeiner, S. (2000). CREB couples neurotrophin signals to survival messages. *Neuron* 25, 11–14.
- Fiskum, G., Murphy, A.N., and Beal, M.F. (1999). Mitochondria in neurodegeneration: acute ischemia and chronic neurodegenerative diseases. *J. Cereb. Blood Flow Metab.* 19, 351–369.

- Gardoni, F., Bellone, C., Viviani, B., Marinovich, M., Meli, E., Pellegrini-Giampietro, D.E., Cattabeni, F., and Di Luca, M. (2002). Lack of PSD-95 drives hippocampal neuronal cell death through activation of an alpha CaMKII transduction pathway. *Eur. J. Neurosci.* *16*, 777–786.
- Ghosh, A. (2002). Neurobiology. Learning more about NMDA receptor regulation. *Science* *295*, 449–451.
- Greengard, P. (2001). The neurobiology of slow synaptic transmission. *Science* *294*, 1024–1030.
- Hanson, S.K., Grotta, J.C., Waxham, M.N., Aronowski, J., and Ostrow, P. (1994). Calcium/calmodulin-dependent protein kinase II activity in ischemia with reperfusion in rats. *Stroke* *25*, 466–473.
- Hardingham, G.E., Fukunaga, Y., and Bading, H. (2002). Extrasynaptic NMDARs oppose synaptic NMDARs by triggering CREB shut-off and cell death pathways. *Nat. Neurosci.* *5*, 405–414.
- Khanna, S., Roy, S., Park, H.A., and Sen, C.K. (2007). Regulation of c-Src activity in glutamate-induced neurodegeneration. *J. Biol. Chem.* *282*, 23482–23490.
- Kinouchi, H., Epstein, C.J., Mizui, T., Carlson, E., Chen, S.F., and Chan, P.H. (1991). Attenuation of focal cerebral ischemic injury in transgenic mice overexpressing CuZn superoxide dismutase. *Proc. Natl. Acad. Sci. USA* *88*, 11158–11162.
- Krupp, J.J., Vissel, B., Thomas, C.G., Heinemann, S.F., and Westbrook, G.L. (1999). Interactions of calmodulin and  $\alpha$ -actinin with the NR1 subunit modulate Ca<sup>2+</sup>-dependent inactivation of NMDA receptors. *J. Neurosci.* *19*, 1165–1178.
- Krajewski, S., Krajewska, M., Ellerby, L.M., Welsh, K., Xie, Z., Deveraux, Q.L., Salvesen, G.S., Bredesen, D.E., Rosenthal, R.E., Fiskum, G., and Reed, J.C. (1999). Release of caspase-9 from mitochondria during neuronal apoptosis and cerebral ischemia. *Proc. Natl. Acad. Sci. USA* *96*, 5752–5757.
- Lipton, S.A. (2006). Paradigm shift in neuroprotection by NMDA receptor blockade: memantine and beyond. *Nat. Rev. Discov.* *5*, 160–170.
- Liu, L., Lau, L., Zhu, D.Y., Wei, J.S., Zou, S., Sun, H.S., Fu, Y.P., Liu, F., and Lu, Y. (2004). Expression of Ca<sup>2+</sup>-permeable AMPA receptor channels primes cell death in transient forebrain ischemia. *Neuron* *43*, 43–55.
- Liu, Y., Wong, T.P., Aarts, M., Rooyackers, A., Liu, L., Lai, T.W., Wu, D.C., Lu, J., Tymianski, M., Craig, A.M., and Wang, Y.T. (2007). NMDA receptor subunits have differential roles in mediating excitotoxic neuronal death both *in vitro* and *in vivo*. *J. Neurosci.* *27*, 2846–2857.
- Lisman, J., Schulman, H., and Cline, H. (2002). The molecular basis of CaMKII function in synaptic and behavioural memory. *Nat. Rev. Neurosci.* *3*, 175–190.
- Lo, E.H., Dalkara, T., and Moskowitz, M.A. (2003). Mechanisms, challenges and opportunities in stroke. *Nat. Rev. Neurosci.* *4*, 399–415.
- Mabuchi, T., Kitagawa, K., Kuwabara, K., Takasawa, K., Ohtsuki, T., Xia, Z., Storm, D., Yanagihara, T., Hori, M., and Matsumoto, M. (2001). Phosphorylation of cAMP response element-binding protein in hippocampal neurons as a protective response after exposure to glutamate *in vitro* and ischemia *in vivo*. *J. Neurosci.* *21*, 9204–9213.
- Madden, D.R. (2002). The structure and function of glutamate receptor ion channels. *Nat. Rev. Neurosci.* *3*, 91–101.
- Marshall, J., Dolan, B.M., Garcia, E.P., Sathe, S., Tang, X., Mao, Z., and Blair, L.A. (2003). Calcium channel and NMDA receptor activities differentially regulate nuclear C/EBP $\beta$  levels to control neuronal survival. *Neuron* *39*, 625–639.
- Omkumar, R.V., Kiely, M.J., Rosenstein, A.J., Min, K.T., and Kennedy, M.B. (1996). Identification of a phosphorylation site for calcium/calmodulin-dependent protein kinase II in the NR2B subunit of the N-methyl-D-aspartate receptor. *J. Biol. Chem.* *271*, 31670–31678.
- Pellegrini-Giampietro, D.E., Gorter, J.A., Bennett, M.V., and Zukin, R.S. (1997). The GluR2 (GluRB) hypothesis: Ca<sup>2+</sup>-permeable AMPA receptors in neurological disorders. *Trends Neurosci.* *20*, 464–470.
- Peng, P.L., Zhong, X.F., Tu, W.H., Soundarapandian, M.M., Molner, P., Zhu, D.Y., Liu, S.H., and Lu, Y. (2006). ADAR2-Dependent RNA Editing of AMPA Receptor Subunit GluR2 Determines Vulnerability of Neurons in Forebrain Ischemia. *Neuron* *49*, 719–733.
- Petersen, J.D., Chen, X., Vinade, L., Dosemeci, A., Lisman, J.E., and Reese, T.S. (2003). Distribution of postsynaptic density (PSD)-95 and Ca<sup>2+</sup>/calmodulin-dependent protein kinase II at the PSD. *J. Neurosci.* *23*, 11270–11278.
- Rossi, D.J., Oshima, T., and Attwell, D. (2000). Glutamate release in severe brain ischemia is mainly by reversed uptake. *Nature* *403*, 316–321.
- Salter, M.W., and Kalia, L.V. (2004). Src kinases: a hub for NMDA receptor regulation. *Nat. Rev. Neurosci.* *5*, 317–328.
- Schumacher, A.M., and Schavocky, J.P. (2004). Velentza, A. V., Mirzoeva, S. & Waterson, D. M. A calmodulin-regulated protein kinase linked to neuron survival is a substrate for the calmodulin-regulated death-associated protein kinase. *Biochemistry* *43*, 8116–8124.
- Simon, R.P., Swan, J.H., and Meldrum, B.S. (1984). Blockade of N-methyl-D-aspartate receptors may protect against ischemic damage in the brain. *Science* *226*, 850–852.
- Simpkins, K.L., Guttman, R.P., Dong, Y., Chen, Z., Sokol, S., Neumar, R.W., and Lynch, D.R. (2003). Selective activation induced cleavage of the NR2B subunit by calpain. *J. Neurosci.* *23*, 11322–11331.
- Shohat, G., Spivak-Kroizman, T., Cohen, O., Bialik, S., Shani, G., Berrisi, H., Eisenstein, M., and Kimchi, A. (2001). The pro-apoptotic function of death-associated protein kinase is controlled by a unique inhibitory autophosphorylation-based mechanism. *J. Biol. Chem.* *276*, 47460–47467.
- Sprengel, R., Suchanek, B., Amico, C., Brusa, R., Burnashev, N., Rozov, A., Hvalby, O., Jensen, V., Paulsen, O., Andersen, P., et al. (1998). Importance of the intracellular domain of NR2 subunits for NMDA receptor function *in vivo*. *Cell* *92*, 279–289.
- Sun, M.K., Hongpaisan, J., Nelson, T.J., and Alkon, D.L. (2008). Poststroke neuronal rescue and synaptogenesis mediated *in vivo* by protein kinase C in adult brains. *Proc. Natl. Acad. Sci. USA* *105*, 13620–13625.
- Takasu, M.A., Dalva, M.B., Zigmond, R.E., and Greenberg, M.E. (2002). Modulation of NMDA receptor-dependent calcium influx and gene expression through EphB receptors. *Science* *295*, 491–495.
- Thomas, C.G., Miller, A.J., and Westbrook, G.L. (2006). Synaptic and extrasynaptic NMDA receptor NR2 subunits in cultured hippocampal neurons. *J. Neurophysiol.* *95*, 1727–1734.
- Tovar, K.R., and Westbrook, G.L. (1999). The incorporation of NMDA receptors with a distinct subunit composition at nascent hippocampal synapses *in vitro*. *J. Neurosci.* *19*, 4180–4188.
- Uehara, T., Nakamura, T., Yao, D., Shi, Z.Q., Gu, Z., Ma, Y., Masliah, E., Nomura, Y., and Lipton, S.A. (2006). S-nitrosylated protein-disulphide isomerase links protein misfolding to neurodegeneration. *Nature* *441*, 513–517.
- Van Eldik, L.J. (2002). Structure and enzymology of a death-associated protein kinase. *Trends Pharmacol. Sci.* *23*, 302–304.
- Velentza, A.V., Schumacher, A.M., Weiss, C., Egli, M., and Watterson, D.M. (2001). A protein kinase associated with apoptosis and tumor suppression: structure, activity, and discovery of peptide substrates. *J. Biol. Chem.* *276*, 38956–38965.
- Wang, J., Liu, S.H., Fu, Y.P., Wang, J.H., and Lu, Y. (2003a). Cdk5 activation induces CA1 pyramidal cell death by direct phosphorylation of NMDA receptors. *Nat. Neurosci.* *6*, 1039–1047.
- Wang, J., Liu, S., Haditsch, U., Tu, W., Cochrane, K., Ahmadian, G., Tran, L., Paw, J., Wang, Y., Mansuy, I., et al. (2003b). Interaction of calcineurin and type-A GABA receptor gamma 2 subunits produces long-term depression at CA1 inhibitory synapses. *J. Neurosci.* *23*, 826–836.
- Wang, H.G., Pathan, N., Ethell, I.M., Krajewski, S., Yamaguchi, Y., Shibasaki, F., McKeon, F., Bobo, T., Franke, T.F., and Reed, J.C. (1999). Ca<sup>2+</sup>-induced apoptosis through calcineurin dephosphorylation of BAD. *Science* *284*, 339–343.
- Waxham, M.N., Grotta, J.C., Silva, A.J., Strong, R., and Aronowski, J. (1996). Ischemia-induced neuronal damage: a role for calcium/calmodulin-dependent protein kinase II. *J. Cereb. Blood Flow Metab.* *16*, 1–6.
- Xiong, Z.G., Zhu, X.M., Chu, X.P., Minami, M., Hey, J., Wei, W.L., MacDonald, J.F., Wemmie, J.A., Price, M.P., Welsh, M.J., and Simon, R.P. (2004). Neuroprotection in ischemia: blocking calcium-permeable acid-sensing ion channels. *Cell* *118*, 687–698.

## EXTENDED EXPERIMENTAL PROCEDURES

### Focal Cerebral Ischemia and Transient Global Ischemia

In brief, a 7/0 surgical nylon monofilament with rounded tip was introduced into the left internal carotid through the external carotid stump, and advanced 10–13 mm past the carotid bifurcation. Occlusion was confirmed when blood flow was reduced by at least 80% of the baseline. The filament was left in place for 60 min or 120 min and then withdrawn. The sham-operated animals were treated identically, except that the middle cerebral artery was not occluded after the neck incision. 24 hr after reperfusion, brain was removed rapidly and frozen at  $-20^{\circ}\text{C}$  for 5 min. Coronal slices were made at 1 mm from the frontal tips, and sections were immersed in 2% 2,3,5-triphenyltetrazolium chloride (TTC) at  $37^{\circ}\text{C}$  for 20 min. The presence or absence of infarctions was determined by examining TTC-stained sections for the areas that did not stain with TTC. The infarct size was expressed as the percentage of the coronal section area. Neurological deficits of the experimental animals throughout the 24 hr period after MCAO were graded on a scale of 0 to 5. The criteria were as follows: grade 0, no observable neurological deficits; grade 1, failed to extend right forepaw; grade 2, circled to the right; grade 3, fell to the right; grade 4, could not walk spontaneously; and grade 5, dead. Transient global ischemia was performed as our described before (Wang et al., 2003a; Liu et al., 2004; Peng et al., 2006).

All variance values in the text and figure legends are represented as SEM. Regional differences for infarctions were compared and the numbers of FJ-labeled cells were analyzed using a two-tailed t test. In some studies, one-way analysis of variance (ANOVA) followed by Newman–Keuls post hoc analysis were used. A statistical difference was determined by a value of  $p < 0.01$ .

### Whole-Cell Patch Clamp Recordings

For whole-cell patch clamp recordings (tight-seal  $> 10\ \text{G}\Omega$ ) from CA1 pyramidal cells, hippocampal slices were visualized with IR-DIC using an Axioskop 2FS equipped with Hamamatsu C2400-07E optics. EPSCs were evoked by stimulating the Schaffer-collateral fibers. The location of the stimulus electrode (bipolar tungsten electrode) was at the Schaffer collateral pathway about  $60\ \mu\text{m}$  from CA1 pyramidal cell bodies. Stimulus intensities in all experiments were set to 40% of the maximum response of EPSCs. Stimuli were delivered at a frequency of 0.1 Hz. The intracellular solution contained (in mM) 142.5 Cs-gluconate, 7.5 CsCl, 10 HEPES, 0.2 EGTA, 2 Mg-ATP, 0.3 GTP (pH 7.4, 296 mOsm). The currents were filtered at 5 kHz.

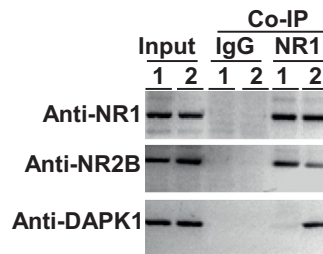


**Figure S1. Constitutively Active DAPK1 Binds with NR2B Subunit, Relates to Figure 1**

Cell lysates (500  $\mu$ g proteins) from the HEK293 cells coexpressing the recombinant NR1/NR2B with wild-type DAPK1 (lane 1) or constitutively active DAPK1 (lane 2) were precipitated with non-specific IgG (IgG) or anti-NR1 (NR1) and probed with anti-NR1, anti-NR2B (or NR2A), or anti-DAPK1. Input: 10  $\mu$ g of protein was loaded in each lane. Similar results were observed in each of the three experiments.

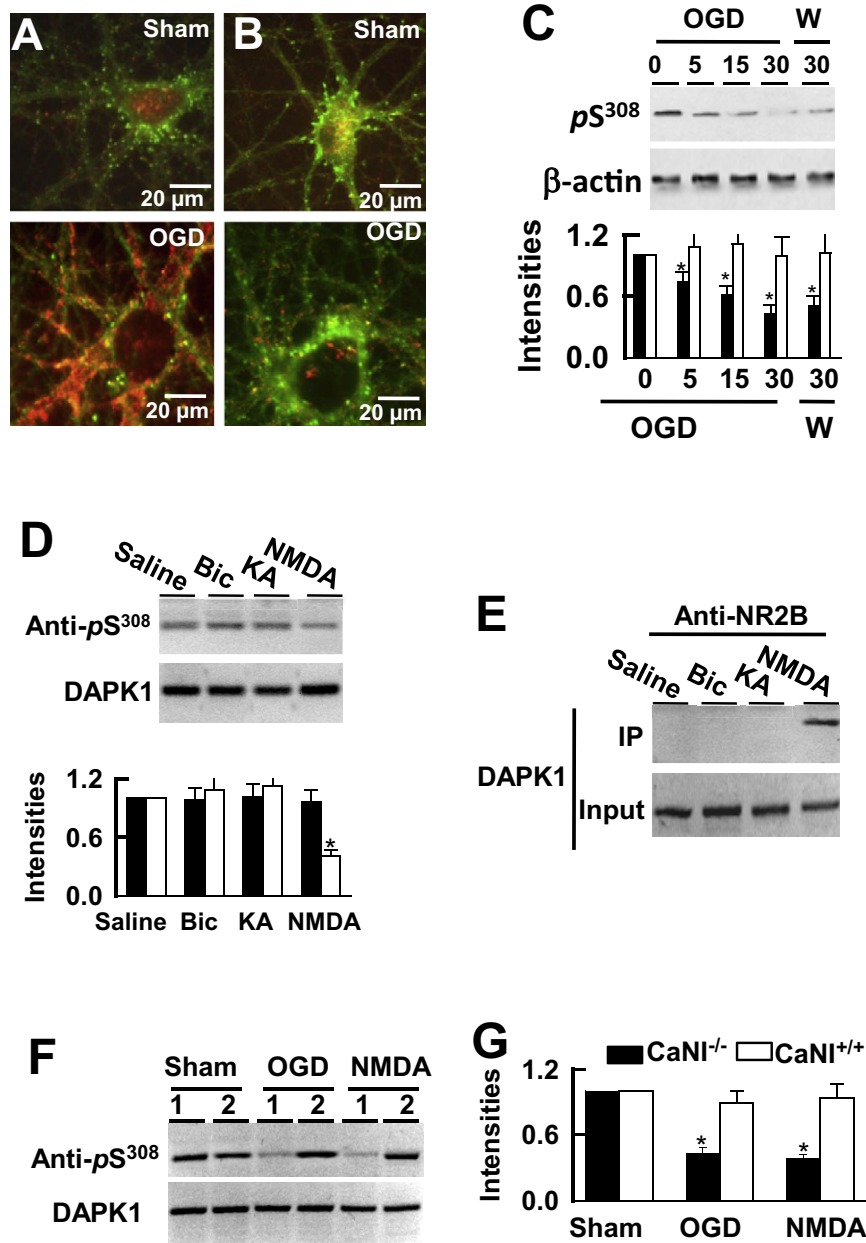


**Figure S2. CaN Activates DAPK1 in Response to Ischemia, Relates to Figure 5**

(A and B) Representative images of the cultures (DIV18) from DAPK1<sup>+/+</sup> (A) and DAPK1<sup>-/-</sup> (B) mice. The cultures were exposed to OGD for 0 min (sham) or 30 min (OGD). 5 min after OGD washout these cultures were costained with anti-pMLC (red) and anti-F-actin (green). Similar results were observed in each of the four experiments.

(C) DAPK1<sup>+/+</sup> neuronal cultures (DIV18) were exposed to OGD for 0, 5, 15, or 30 min. Immediately after OGD (OGD) or 30 min after OGD washout (w) the extracts were prepared and blotted with anti-pS<sup>308</sup> or anti- $\beta$ -actin, as indicated. The intensities of the anti-pS<sup>308</sup> (filled bars) and anti- $\beta$ -actin (open bars) blots were normalized to their respective signals at 0 min OGD (defined as 1.0). Data are summarized in bar graph (n = 4, \*p < 0.01).

(D) DAPK1<sup>+/+</sup> neuronal cultures (DIV18) were exposed to saline, or 10  $\mu$ M bicuculline (bic), or 50  $\mu$ M NMDA/10  $\mu$ M glycine for 30 min. DAPK1 protein was immunoprecipitated and blotted with anti-pS308 or anti-DAPK1. Similar results were seen in each of four experiments.

(E) DAPK1<sup>+/+</sup> neuronal cultures (DIV18) were exposed to saline, or 10  $\mu$ M bicuculline (bic), or 50  $\mu$ M NMDA/10  $\mu$ M glycine for 30 min. Anti-NR2B precipitates were blotted with anti-DAPK1. Input: 20  $\mu$ g of protein without IP was loaded directly.

(F and G) CaNI<sup>+/+</sup> (lane 1) and CaNI<sup>-/-</sup> (lane 2) neuronal cultures were exposed to sham control or OGD or 50  $\mu$ M NMDA/10  $\mu$ M glycine for 30 min. Anti-DAPK1 precipitates were blotted with anti-pS<sup>308</sup> or anti-DAPK1 (F). Data are summarized in bar graph (G, n = 4 per group, \*p < 0.01).

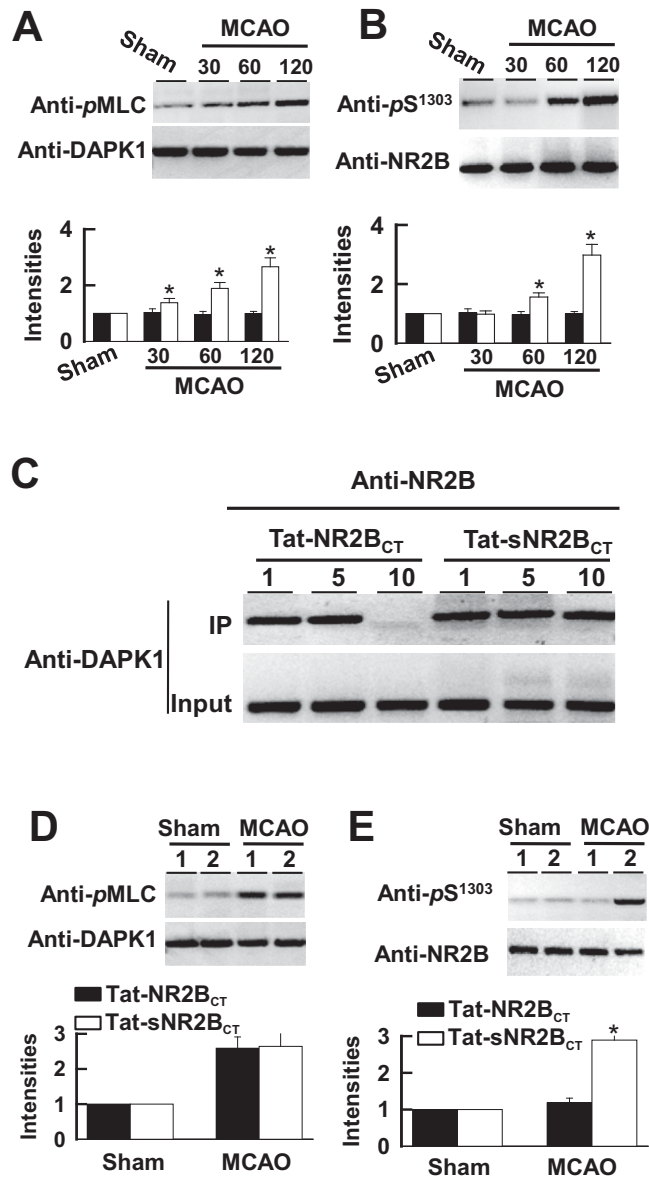


**Figure S3. Tat-NR2B<sub>CT</sub> Blocks DAPK1-NMDA Receptor Association, Relates to Figure 7**

(A and B) DAPK1 activation is associated with NR2B phosphorylation at Ser-1303 after MCAO. The adult male DAPK1<sup>+/+</sup> mice were operated for MCAO or sham for 60 min. 30, 60, or 120 min after reperfusion the cortical membrane extracts were then prepared and precipitated with anti-DAPK1 (A) or anti-NR1 (B) and blotted with anti-bodies, as indicated. The intensities of the blots were normalized to their respective sham (defined as 1.0). Summarized data are shown in bar graphs. Data are mean ± SEM (n = 6 mice/group, \*p < 0.01).

(C) Uncoupling an activated DAPK1 from NMDA receptor complex by Tat-NR2B<sub>CT</sub>. The adult male DAPK1<sup>+/+</sup> mice were operated for MCAO for 60 min. 60 min after reperfusion, animals were received a single injection (1, 5, 10 mg/kg, *i.v.*) of Tat-NR2B<sub>CT</sub>, Tat-sNR2B<sub>CT</sub> or saline. 60 min after the injection (120 min after MCAO), the forebrain membrane extracts were then prepared and precipitated with anti-NR2B antibody and blotted with anti-DAPK1 (IP). Input: 20 μg of protein without IP was loaded directly. Similar results were observed in each of four experiments.

(D and E) Administration of Tat-NR2B<sub>CT</sub> does not affect DAPK1 activation (D) but eliminates NR2B phosphorylation at Ser-1303 (E). The adult male DAPK1<sup>+/+</sup> mice were received a single injection (10 mg/kg, *i.v.*) of Tat-NR2B<sub>CT</sub> (lane 1) or Tat-sNR2B<sub>CT</sub> (lane 2) 30 min after the injection animals were operated for MCAO or sham for 60 min. 120 min after reperfusion the cortical membrane extracts were prepared and precipitated with anti-DAPK1 (D) or anti-NR1 (E) and blotted with anti-bodies. The intensities of the blots were normalized to their respective sham (defined as 1.0). Summarized data are shown in bar graphs. Data are mean ± SEM (n = 6 mice/group, \*p < 0.01).